Effect of sterilization on 3D printed patient-specific surgical guides

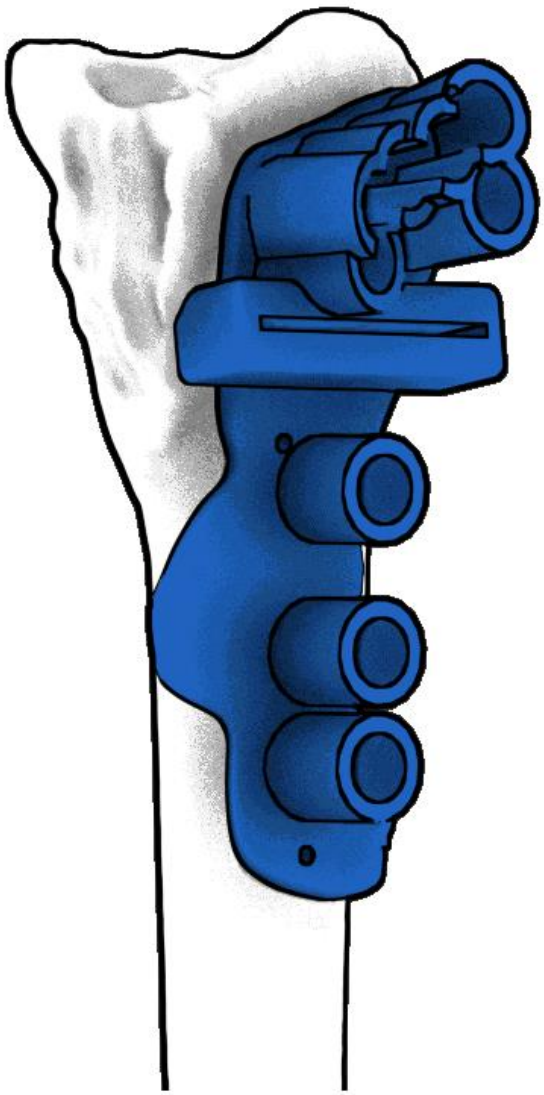

V.H.A.M. van Dal

Technical Medicine – Master Thesis

Delft University of Technology

25-02-2021

EFFECT OF STERILIZATION ON 3D PRINTED PATIENT-SPECIFIC SURGICAL GUIDES

- a template of the official frontpage -

Vito van Dal
Student number : 4374169
25 Feb 2021

Thesis in partial fulfillment of the requirements for the joint degree of Master of Science in
Technical Medicine
University Leiden ; Delft University of Technology ; Erasmus University Rotterdam

Master thesis project (TM30004 ; 35 ECTS)
Dept. of Biomechanical Engineering, TUDELFT
June 2020 – February 2021
Supervisor(s):
Drs. Mike Bemelman
Dr. Jie Zhou
Dr. Jan Heyligers
Drs. Lars Brouwers

Thesis committee members:
Prof. dr. ir. Jaap Harlaar, TU Delft (chair)
Drs. Mike Bemelman, ETZ Tilburg
Dr. Jie Zhou, TU Delft
Dr. Jan Heyligers, ETZ Tilburg
Drs. Lars Brouwers, ETZ Tilburg

Universiteit Leiden
TU Delft Delft University of Technology
Erasmus Universiteit Rotterdam

Abstract

Background

The current workflow for the design and production of patient-specific surgical guides at the Elisabeth-TweeSteden hospital is out-sourced to external companies, making it a time-consuming and costly task. In order to minimize the production time and expenses, the design and fabrication of these guides could be implemented into the hospital's workflow using an in-house available 3D printer. Compared to the current gold standard for the production of patient-specific surgical guides, a different printing technique and 3D print material will be used. Therefore, it should be determined whether these are suitable for the production of the guides. Moreover, the 3D printed models must be compatible with the in-house sterilization method in order to ensure quality and reliability. The aim of this thesis was to investigate the effect of the in-house available sterilization method on the mechanical, dimensional, and sterility properties of a novel biocompatible 3D printing material.

Methods and results

BioMed Clear resin specimens were tested according to the ISO standards for mechanical testing of plastics. The specimens were printed with the Form 2 printer using the stereolithography (SLA) print technique. Overall, steam sterilization changed the mechanical properties of the material, making it stronger and stiffer but more brittle, as compared to unsterilized specimens. The dimensional tests indicated that sterilization resulted in a dimensional change, up to 0.12 mm, which mostly occurred in the small crevices of the model. The deviations of the dimensions of the resulting 3D printed model compared to the digital 3D model were roughly less than 0.3 mm, which is comparable to the accuracy of the gold standard material, polyamide 12. Sterility tests showed that sterilization of the 3D printed models is indeed mandatory for the guides to be used intraoperatively. Also, the Central Sterile Services Department of the hospital is able to deliver sterile medical devices that can be stored for a minimum of four weeks at the sterile storage room.

Conclusion

With the feasibility confirmed for the hospital to be able to design and produce patient-specific surgical guides in-house, it is necessary to stress that the hospital must meet the Medical Device Regulations by complying with an appropriate quality management system, documenting the manufacturing process, evaluating the performance, and reviewing the experiences from clinical use.

List of contents

Introduction

Sterilization of medical devices

In 2017, healthcare institutions in the Netherlands performed over 3.1 million surgical procedures (1). With an increasing and aging population in the coming years, this number will grow even further. All such invasive procedures require direct contact of medical devices and instruments with the patient's sterile tissues or mucous membranes (2). This direct contact involves significant risks in introducing pathogenic microorganisms that can cause an infection. So-called Healthcare-associated Infections (HAIs) can be significantly reduced by the proper use of disinfection and sterilization procedures for medical devices. In case a medical device is inadequately sterilized, it poses the risk of generating infections via a person-to-person or environmental transmission (3). Therefore, disinfection and sterilization of medical devices for operational procedures is of great importance.

To decide whether medical devices and instruments should be sterilized or disinfected before their use, a classification scheme that was introduced by H. Spaulding in the late 1960s is still being used nowadays. This classification scheme divides medical devices into three different groups based on the level of risk of generating infections that come with their intended use, namely: *critical, semi-critical, and non-critical devices (4)*.

Critical devices carry the highest potential for generating infections once contaminated with any microorganism, including bacterial spores (3). These devices can come in contact with the patient's sterile tissues. Therefore, it is of utmost importance that these devices are sterilized before their use. In this category, devices include surgical instruments, implants, catheters for cardiological or urological interventions, and ultrasound probes for sterile applications (5).

Semi-critical devices are defined as those that will likely touch disrupted skin or mucous membranes; however, they do not contact sterile tissues. Examples of semi-critical medical devices are respiratory equipment, non-invasive endoscopes, laryngoscope blades, and urinal bottles (6). A limited number of bacterial spores are acceptable, but all other microbial life forms should be eliminated. The fact that bacterial spores are acceptable on semi-critical medical devices is based on mucous membranes' resistance and non-intact skin against these pathogens. However, these different tissue types are prone to infection by other microorganisms, such as viruses, bacteria, and mycobacteria (3).

Non-critical devices represent the lowest risk of contamination as they will not come into contact with the patient's sterile tissues or mucous membranes. Non-critical devices can be used on intact skin only. Examples of the devices that are categorized as non-critical are stethoscopes, the cuffs of blood pressure monitors, and oximeters. Most microorganisms cannot penetrate intact skin, so that sterilization of non-critical devices is not necessary. Non-critical medical devices can be processed using low-level disinfection, such as ethyl or isopropyl alcohol (70-90%).

There are several forms of sterilization for medical devices. Among the most widely used method is steam sterilization with an autoclave because of its large margin of safety due to its consistency, reliability, and lethality (3). Steam sterilization can be used on most medical and surgical devices as most of them are made of heat-stable materials. However, the introduction of new materials (e.g., plastics) for medical devices that cannot withstand the heat and moisture of steam sterilization has required the development of low-temperature sterilization methods (e.g., ethylene oxide gas, hydrogen peroxide gas plasma, and ozone sterilization). To choose the best-suited sterilization method for a medical device, one should consider the material composition, its intended use, and its classification.

Sterilization of 3D printed models

Three-dimensional (3D) printing, also known as additive manufacturing, has been a rapidly advancing technology since the 1980s. It is comprised of different techniques, such as Fused Deposition Modelling (FDM), Stereolithography (SLA), Selective Laser Sintering (SLS), PolyJet Technology, and Digital Light Processing (DLP) (7). These techniques use the

material to build up a model layer by layer. Due to improvements and innovations in 3D printing, these techniques have become easier to utilize, less expensive, and more readily available (8). Combined with the use of Computer-Aided Design (CAD) software and Standard Tessellation Language (STL) models, 3D printing can be used to create physical models from a wide variety of materials, such as polylactic acid (PLA) (9). 3D printing has created enormous opportunities for various industries, such as the healthcare industry, where it has contributed to innovations in treatment strategies

Implementing 3D printing in a healthcare setting can have many implications, diversifying from treatment planning or the production of surgical guides to printing supporting materials for tissue engineering or even printing tissues for organ regeneration (10, 11). The clinical application of the 3D models, such as surgical jigs and guides, is categorized as critical when they are likely to contact the patients' sterile tissues. Therefore, sterilization of 3D printed objects for intraoperative use is mandatory. As many materials used in 3D printing are heat-sensitive, the use of steam sterilization or dry heat sterilization might damage their morphological, mechanical, and functional properties. Therefore, the sterilization method should be carefully addressed to be reliable, practical, and safe for 3D printed objects (12).

Clinical problem

At the Elisabeth-Two Cities Hospital, the current workflow for the design and fabrication of patient-specific surgical guides is out-sourced to external companies. Therefore, the design and fabrication phases are time-consuming and costly. To minimize the production time and expenses, the hospital could implement the design and fabrication of surgical guides in the hospital's workflow using an in-house available 3D printer. The current gold standard for producing patient-specific surgical guides is selective laser sintering (SLS) printing with Polyamide 12 (PA12). As SLS printing requires large investments for the production of surgical guides, there was a need to perform investigations to determine whether stereolithography (SLA) 3D printing with an in-house available 3D printer could take over out-sourcing tasks. SLA printers use a laser to UV cure specific areas of a resin tank to form a substantial part on one cross-section at a time.

BioMed Clear resin was chosen as the material to be tested as the manufacturer stated that it should be compatible with several sterilization methods, including steam sterilization. Moreover, the material is a biocompatible USP Class VI certified material suitable for long-term skin or mucosal membrane contact. Other resins from this manufacturer are either not biocompatible or can only be used for other applications, such as the dental industry.

Research Goal

This research aimed to investigate whether the in-house available 3D printer would be suited for the production of patient-specific surgical guides for operational usage. For this purpose, tests were performed to understand how the 3D prints would react to in-house sterilization with steam. To this end, three different types of tests were performed on the chosen biocompatible resin material.

Thesis outline

First, In part A, the effect of the in-house steam sterilization method on a 3D print material's mechanical properties will be presented. The results obtained from three different mechanical tests will be reported, namely: tensile tests, flexural tests, and impact tests. In Part B, the in-house steam sterilization method's effect on the dimensional accuracy of surgical guides will be shown. In Part C, the results obtained from the sterility tests of 3D printed specimen groups, with and without exposure to bacterial contamination, after the 3D printing process and after sterilization, will be given. In addition, a cost-benefit analysis is provided in the general discussion where in-house design and production of the surgical guides are contrasted with out-sourcing. Furthermore, the laws and regulations regarding the in-house production of patient-specific surgical guides are elucidated.

To determine whether BioMed clear resin would be comparable to the current gold standard material for patient-specific surgical guides (PA12), the effect of the in-house steam sterilization procedure on the 3D print material was investigated. In Table 1, the various tests performed are divided into three parts. In the materials and methods section, the reference codes are used to indicate which type of tests is concerned with.

Table 1. The various tests that were performed. They are divided into mechanical tests (Part A), dimensional tests (Part B), and sterilization tests (Part C).

Test type	Material property tests	Reference code
Mechanical (Part A)	Flexural	ISO 178
	Impact (Charpy)	ISO 179
	Tensile	ISO 527
Dimensional (Part B)	Accuracy	
Sterilization (Part C)	Sterility	

Part A – Mechanical tests

Materials & methods

Equipment and materials

In this study, we chose to investigate the effect of steam sterilization on the mechanical behavior of two different 3D print materials, namely, Pearl-White PLA and Biomed Clear resin, for comparison purposes. Two in-house available 3D printers were utilized to fabricate the test specimens that were divided into groups, as shown in Table 2.

Table 2. Printer settings for the different study groups in mechanical tests.

Group	Material	Infill percentage (%)	Print Orientation (degrees)
A1	PLA Pearl White	60	0
A2	PLA Pearl White	60	90
A3	PLA Pearl White	100	0
A4	PLA Pearl White	100	90
A5	BioMed Clear Resin	100	0
A6	BioMed Clear Resin	100	45

In group A1-A4, specimens were printed with the Ultimaker S5 printer (Ultimaker B.V., Utrecht, The Netherlands) in Pearl White PLA with a 0.4 mm print core A.A. nozzle. Water-soluble Polyvinyl Alcohol (PVA) was used as a support material for specimens printed at 90 degrees rotation relative to the build plate. Table 2 shows the printer settings used in Cura 4.7.0 (Ultimaker, Utrecht, The Netherlands) for each group. In group A5-A6, specimens were printed with the Form 2 printer (Formlabs Inc., Somerville, MA, USA) in Biomed Clear V1 resin, a medical-grade resin for biocompatible applications requiring long-term skin or mucosal contact. The software, PreForm v. 3.8.1 (Formlabs Inc., Somerville, MA, USA), was used as the print preparation software to orientate the specimens on the build platform. A layer thickness of 0.1 mm was set for printing, which was the same for the PLA specimens. Supports were generated using the auto-generation feature in this software. Printer settings for the Form 2 printer are shown in Table 2.

Computer-Aided Design (CAD) modeling

ISO 178 – Flexural test specimen

The computer-aided design (CAD) of specimens was performed in SolidWorks according to the ISO 178 standard for the determination of flexural properties of plastics. Specimens were designed to be 80 mm x 10 mm x 4 mm and are shown in Figure 1. Specifications and the dimensions are shown in Table 3. For each specimen group, six specimens were printed, which resulted in 72 specimens in total.

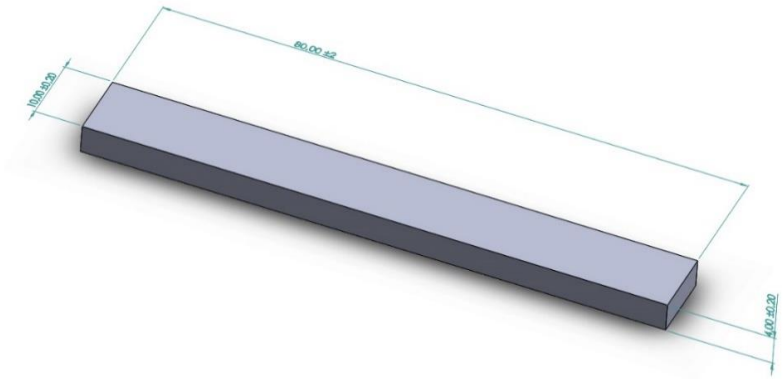

Figure 1. Digital model of an ISO 178 specimen visualized in SolidWorks. The dimensions are 80 mm x 10 mm x 4 mm.

Table 3. Specifications of specimens for ISO 178 flexural tests. Dimensions are in millimeters.

		Dimensions [mm]
l	Length of specimen	80 ± 2
b	Width of specimen	10.0 ± 0.2
h	Thickness of specimen	4.0 ± 0.2
R_1	Radius of the loading edge	5.0 ± 0.2
R_2	Radius of supports	5.0 ± 0.2
L	Length of the span between supports [a]	64
[a] Distance between the points of contact between the test specimen and the test specimens supports		

ISO 179 – Charpy impact test specimen

Specimens were designed in SolidWorks (Waltham, MA, USA) according to the ISO 179 standard for the determination of Charpy notched impact properties of plastics. Dimensions of the 3D printed specimens were 80 mm x 10 mm x 4 mm. Illustrations of the specimens and their dimensions are shown in Figure 2 and Table 4.

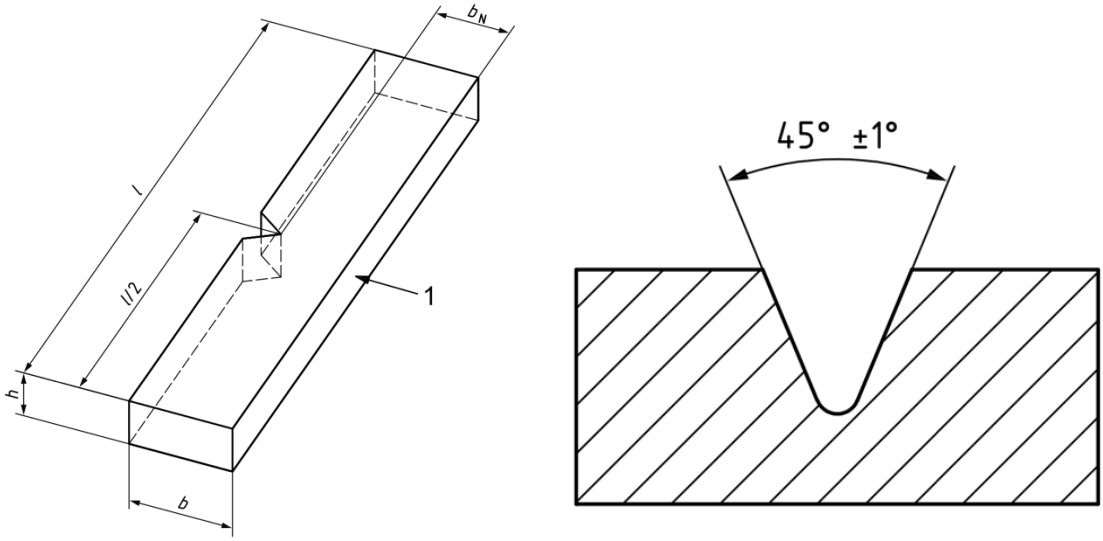

Figure 2. On the left, Charpy notched impact specimen. ''1' indicates the line of the impact of the pendulum swing to the specimen. On the right, the cross-section of the notch of the specimen is visualized.

Table 4. Specifications of specimens for ISO 179 tests. Dimensions are in millimeters.

	Specimen properties	**Dimensions [mm]**
l	Length	80 ± 2
b	Width	10.0 ± 0.2
h	Thickness	4.0 ± 0.2
L	Span[a]	40
	Notch type	A
r_N	Notch tip radius, r_N	0.25 ± 0.05
b_N	Remaining width, b_N, at notch tip	8.0 ± 0.2
[a] Preferred span width for the specimens is 62 mm. This span was not available for the Zwick pendulum impact tester.		

ISO 527 – Tensile test specimen

The computer-aided design (CAD) of the samples was performed in SolidWorks (Waltham, MA, USA) according to the ISO 527-2 standard for tensile testing of plastics. Specimens were designed to be 4 mm thick and 170 mm long. Specifications of the dimensions are shown in Figure 3 and Table 5. The specimen's CAD files were exported in the standard tessellation language (STL) file format for 3D printing.

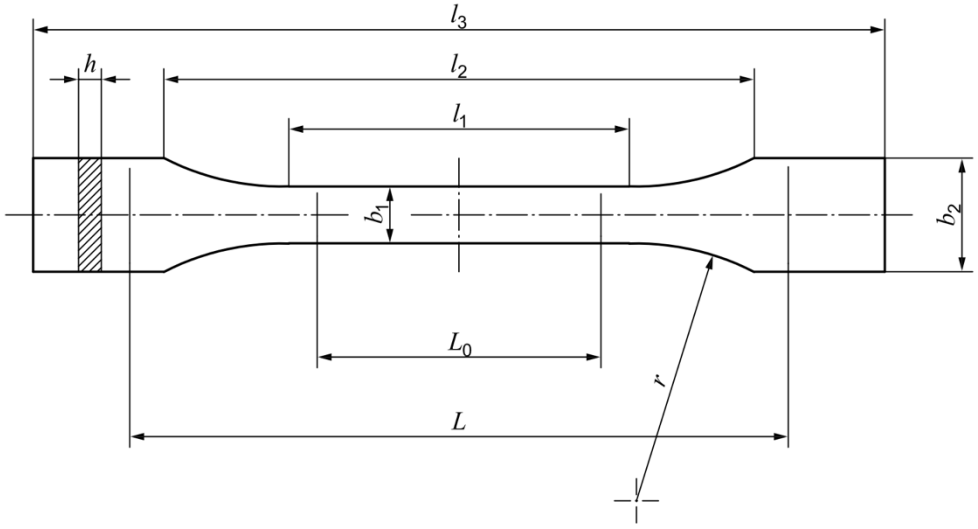

Figure 3. Test specimen for tensile tests.

Table 5. Specifications of specimens for ISO 527 tensile tests. Dimensions are in millimeters.

	Specimen properties	Dimensions [mm]
l_3	Overall length	170
l_1	Length of the narrow parallel-sided portion	80 ± 2
r	Radius	24 ± 1
l_2	Distance between broad parallel-sided portions [a]	109.3 ± 3.2
b_2	Width at ends	20.0 ± 0.2
b_1	Width at narrow portions	10.0 ± 0.2
h	Preferred Thickness	4.0 ± 0.2
L_0	Gauge length (preferred) [b]	75.0 ± 0.2
L	The initial distance between grips	115 ± 1

[a] $l_2 = l_1 + [4r(b_2 - b_1) - (b_2 - b_1)^2]^{1/2}$, resulting from l_1, r, b_1 and b_2, but within the indicated tolerances
[b] used for extensometer placement, however, not used in this study

3D printing of test specimens

The STL files of the samples were imported in the slicing software of both 3D printers. The automatic placement feature was used for the best orientation of the test samples on the build platform. The models printed with the Ultimaker S5 printer were printed in two different print orientations, as shown in Figure 4. ISO 527 specimens were used as examples to illustrate the orientation of the specimens on the build platform. Type A was called the 0 degrees orientation, and type B was called the 90 degrees orientation. Type A samples did not require the addition of PVA support structures. On the contrary, for type B specimens, PVA support structures were supplemented. In Table 6, the printer settings for all the groups are summarized.

Table 6. Printer settings for all the groups. Groups A1-A4 are printed with the Ultimaker S5 (FDM) printer. Groups A5 and A6 are printed with the Form 2 (SLA) printer.

Group	A1	A2	A3	A4	A5	A6
Layer height	0.1 mm	0.1 mm	0.1 mm	0.1 mm	0.1 mm	0.1 mm
Wall thickness	1 mm	1 mm	1 mm	1 mm	/	/
Top/bottom layers	10	10	10	10	/	/
Infill density	60 %	60 %	100 %	100 %	100 %	100 %
Print orientation	0°	90°	0°	90°	0°	45°
Infill pattern	Triangles	Triangles	Triangles	Triangles	/	/
Print temperature	200°C	200°C	200°C	200°C	/	/
Print speed	70 mm/s	70 mm/s	70 mm/s	70 mm/s	/	/
Brim	Yes	Yes	Yes	Yes	/	/
Support density	50%	50%	50%	50%	1.30	1.30
Touchpoint Size	/	/	/	/	0.60 mm	0.60 mm
Samples per group	12	12	12	12	12	12

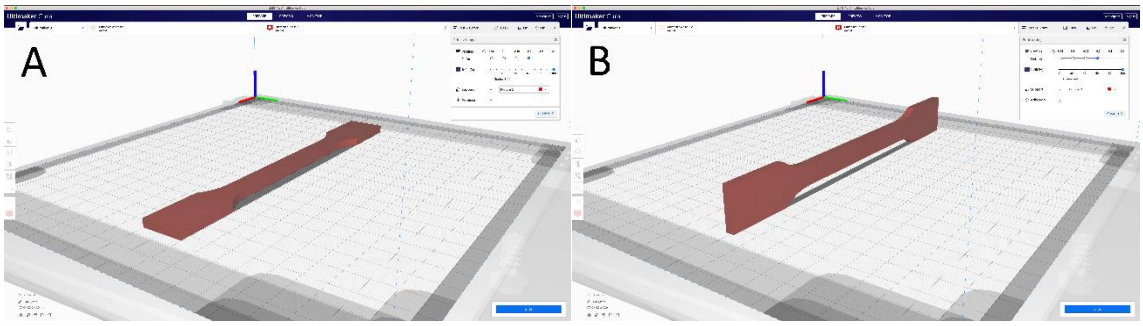

Figure 4. A: Specimen for ISO 527 tensile test visualized on the Ultimaker S5 printer build platform in Cura. This print orientation is called the 0 orientation. B: 90 print orientation of an ISO 527 specimen. This orientation required additional support.

Biomed Clear resin (Formlabs, Somerville, MA, USA) specimens printed with the Form 2 (Formlabs, Somerville, MA, USA) printer were at first only orientated at 0 degrees (Figure 5, type A) due to the limited availability of the medical-grade resin. However, post-processing of the SLA printed models resulted in significant warping of the specimens. Therefore, the specimens were also printed in a 45° tilt in the z-direction, as shown in Figure 5B. The adjusted orientation allowed for a reduction in surface area during printing for each layer and decreased the print's contact area with the tank. A reduction of the surface area means that the print will be subjected to less force as the build platform rises with every layer. The contact area of the Form 2 build platform is 14.5 x 14.5 cm. Therefore, the samples printed at 0 degrees had to be orientated diagonally on the build platform, as shown in Figure 5A. The specimens' orientation at a 45 ° angle allowed for a more efficient production process as five specimens could be printed simultaneously. For each group, a total of 12 specimens were printed, which resulted in 72 specimens in total.

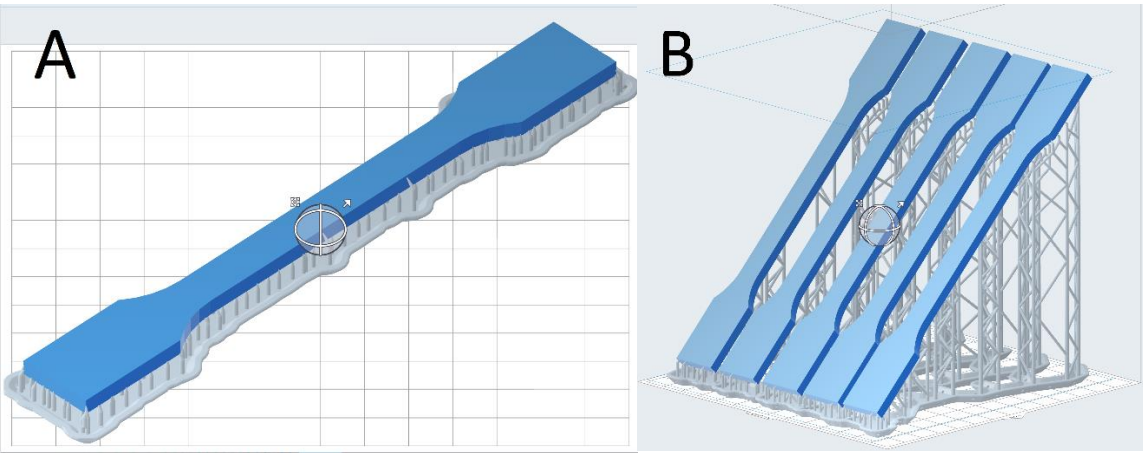

Figure 5. A: specimen for ISO 527 tensile tests visualized on the Form 2 printer build platform in PreForm software. A is called the 0° print orientation. B: 45° print orientation. Supporting structures are visualized in grey and are printed from the same material.

Post-Processing

After the completion of the 3D printing process, the specimens were visually inspected for defects or errors. For PLA specimens in groups A2 and A4, post-processing was necessary to remove the supporting PVA structures with removal tools. Additionally, PLA specimens were processed in a cold water bath to dilute the PVA. Specimens printed with the Form 2 printer were first washed in the Form Wash (Formlabs Inc., Somerville, MA, USA) in 90% isopropyl alcohol (IPA) for 15 minutes to remove any uncured resin from the surface of the print. Additionally, the specimens were post-cured in a heated, rotating chamber at 60°C for 60 minutes in the Form Cure (Formlabs Inc., Somerville, MA, USA) with U.V. radiation according to the manufacturer's instructions. The curing procedure was performed to maximize the material's mechanical properties. Afterwards, the support structures were removed from the specimens with cutting pliers.

Sterilization Method

For each group, half of the samples were sterilized according to Elisabeth-Two Cities Hospital's sterilization process. The sterilization process also included automated cleaning of the specimens in a washing machine (Uniclean PL, MMM Münchener Medizin Mechanik GmbH, Munich, Germany) with neodisher MediClean forte (Dr. Weigert GmbH, Hamburg, Germany) before the sterilization process. This step was also added to the process as it is part of the workflow in the Central Sterile Services Department (CSSD). After the automated washing procedure, models were packed in BOP paper/film pouches (Amcor Flexibles SPS, Coulommiers, France). These pouches are permeable to steam, ethylene oxide (EtO) gas, and formaldehyde gas sterilization. The specimens were then sterilized in a high-speed pre-vacuum autoclave (Selectomat PL, MMM Münchener Medizin Mechanik GmbH, Munich, Germany) at 134 °C for 3.5 minutes. The high-temperature steam inside the autoclave destroys microorganisms via an irreversible process called coagulation and denaturation of enzymes and structural proteins (3). The limited processing time is due to the high pressure and the presence of moisture, which has a significant effect on the coagulation temperature of proteins.

Data collection and assessment of mechanical properties

ISO 178 – Flexural properties

The flexural tests were performed on an ElectroPuls E10000 machine (Instron, Norwood, MA, USA) and with the Console software according to the ISO 178 standard for determining the flexural properties of plastics (Figure 6). Specimens with a rectangular cross-section, resting on two supports, were deflected with a loading edge acting on the specimen midway between the supports. Before testing, the specimens' width and thickness were measured with a caliper (Mitutoyo, Kawasaki, Kanagawa, Japan) at mid-length of the test specimen. It was then placed on the two supports, and a preload of 5N was applied to avoid a curved region at the start of the stress/strain diagram. For preloading, a crosshead speed of 1 mm/min was used. When the preload of 5N was reached, the deflection measurement system was set to zero. The specimen was deflected at a constant rate at midspan until rupture at the specimen's outer surface or until a maximum strain of 5% was reached, whichever occurred first. The maximum deflection for a 5% strain was implemented in the testing machine settings after the first specimen of group 4 was tested, as it reached a strain of 10.8% before fracture. A test speed of 2 mm/min was chosen for the preferred specimen type as this gave a flexural-strain rate as close as possible to 1%/min for the determination of the flexural modulus. During the procedure, the force applied to the specimen and the specimen's deflection at midspan was measured.

Figure 6. Instron Electropuls machine for mechanical tests. In this picture the machine is setup for ISO 178 flexural tests.

To obtain the specimen's deflection accurately without compliance effects of the machine, usage of a deflectometer is recommended. However, a deflectometer was not available at the time of testing. Therefore, crosshead displacement with a compliance correction was used for the determination of the flexural modulus. According to Annex C from the ISO 178 standard, compliance correction was performed using a highly rigid brass reference bar to determine the load string stiffness of the flexural testing machine. The brass reference bar dimensions were 173 mm x 50 mm x 8 mm with a tensile modulus of 100 GPa. The load string stiffness of the testing machine was ~14kN/mm. After the compliance correction of the testing machine, the flexural properties of the materials could be determined.

Flexural stress was calculated with the use of the following equation:

$$\sigma_f = \frac{3FL}{2bh^2}$$

where

σ_f is the flexural stress, in megapascals;
F is the applied force, in newtons;
L is the span, in millimeters;
b is the width of the specimen, in millimeters;
h is the thickness of the specimen, in millimeters.

The flexural strain was calculated with the use of the following equation:

$$\varepsilon_f = \frac{600sh}{L^2}\%$$

where

ε_f is the flexural strain parameter in question, expressed as a percentage;
s is the deflection, in millimeters;
h is the thickness of the test specimen, in millimeters;
L is the span, in millimeters.

The flexural modulus, E_f, was determined by calculating the deflections corresponding to flexural strains of $\varepsilon_{f1} = 0{,}0005$ and $\varepsilon_{f2} = 0{,}0025$ of the stress/strain curve.

ISO 179 – Charpy impact properties

Specimens' notch height (b_N) and width (*h*) were measured with a caliper for impact area calculation. The Charpy impact strength of the 3D printed materials was determined using a pendulum impact tester (Zwick Roell Group, Ulm, Germany) according to the ISO 179 standard (Figure 7). All specimens were tested using a 1 Joule hammer. The hammer was lifted to 160° and released when the specimen was placed on the supports, with the notch facing away from the impact hammer. The support span was 40 mm as there was no support available with a span width of 62 mm, which was recommended. The 40 mm span width could fulfill the relative comparison of Charpy impact properties between the specimen groups. For each specimen, Charpy impact energy was determined by obtaining the reading from the pointer.

Figure 7. Charpy pendulum impact tester from Zwick Roell. The PLA specimen is placed in the middle on the supports and the pendulum is positioned at a 160 degrees relative to the point of impact.

The pendulum impact tester uses a pointer to determine the impact energy of the specimen. This pointer is moved along with the rotation of the pendulum swing until maximum deviation. The pointer then stops at the maximum rotation of the pendulum. The energy of the pendulum swing is also absorbed by friction, including the friction in the pointer. Therefore, the energy loss due to the friction in the pointer was determined using the ISO 13802 standard (Verification of pendulum-testing machines). For the procedure, the machine had to be operated normally, but without using a test specimen, to obtain the first reading, $W_{f,1}$. Then, without resetting the pointer, the pendulum was rereleased from the initial position to obtain a second reading, $W_{f,2}$. These steps were repeated twice, and the means of the three determinations of $W_{f,1}$ and $W_{f,2}$ were calculated. Energy loss due to friction in the pointer was determined by subtracting the mean of the second reading, $W_{f,2}$, from the mean of the first reading, $W_{f,1}$.

$$W_{f,P} = W_{f,1} - W_{f,2}$$

The losses due to air resistance and friction in the bearings were also determined according to the ISO 13802 standard. For the procedure, the pendulum impact tester was used as standard, only without the use of a test specimen to obtain the first reading, $W_{f,2}$. The

pendulum was allowed to continue to swing freely, without the use of the pointer. At the beginning of the pendulum's tenth forward swing, the pointer was repositioned so that the pendulum drove it a few divisions along the scale. The pointer was then used to obtain the reading as $W_{f,3}$. These steps were then repeated twice to determine the means of the three determinations of $W_{f,2}$ and $W_{f,3}$. The energy loss due to air resistance and pendulum bearing friction, $W_{f,AB}$, was then calculated for one swing with the use of the following equation:

$$W_{f,AB} = \frac{W_{f,3} - W_{f,2}}{20}$$

The total energy loss due to friction was calculated with the use of the following equation:

$$W_f = \frac{1}{2}\left[W_{f,AB} + \frac{\alpha_R}{\alpha_0}\left(W_{f,AB} + 2W_{f,P}\right)\right]$$

where

W_f is the energy loss due to friction;
$W_{f,AB}$ is the energy loss due to air resistance and pendulum bearings;
$W_{f,P}$ is the energy loss due to friction in the pointer;
α_0 is the pendulum's starting angle, expressed in degrees;
α_R is the angle of rise, in degrees

The starting angle of the pendulum was 160°, and the angle of rise was 156°. The frictional force of the pendulum impact tester was then calculated to be 0.018 Joules, which is within the 2% maximum permissible limit of losses due to friction when the hammer's nominal potential energy used is 1 Joule.

ISO 527 – Tensile properties

According to the ISO 527 standard, the tensile tests were performed with the ElectroPuls™ E10000 machine (Instron, Norwood, MA, USA) and the Console software (Figure 8). Pretension values of 30 N and 50 N were used for the Biomed Clear models and PLA models, respectively. These pretension values were based on the tensile modulus provided by the manufacturer, which is 2080 MPa for Biomed Clear resin and 3120 MPa for Pearl White PLA. No extensometer was used for the tests as it was not available. Therefore, the displacement between the gripping positions was used to calculate the nominal strain to measure the specimen's deformation. Instead of measuring the displacement between the grips, it is acceptable to record crosshead displacement. The specimens' width and thickness were measured at three different places with a caliper (Mitutoyo, Kawasaki, Kanagawa, Japan) at the central gauge length and averaged. Five specimens were extended along its major longitudinal axis for each group at a constant test speed of 1 mm/min

Figure 8. Instron Electroplus E10000 machine adjusted for ISO 527 tensile testing of 3D printed specimens.

until the specimen fractured. During the procedure, the load sustained by the specimen and the displacement between the grips were measured at a sampling rate of 20 Hz.

Some of the PLA specimens were significantly deformed and could not fit into the tensile testing machine's grips. These specimens were excluded from any further analysis. When the gripping system caused premature fracture at the jaws or squashing, specimens were also excluded.

Statistical analysis

For the specimens in ISO 178 and ISO 527, data from the testing machine was exported in comma-separated values files (.csv) and imported into Microsoft Excel for further processing. For each specimen in these two groups, the stress-strain curve was plotted. The ultimate flexural/tensile strength, flexural/tensile modulus, and strain at break were investigated under the conditions defined. The flexural/tensile modulus of the specimens was determined by taking the slope of the stress-strain curve σ(ε) in the interval between the two strains $\varepsilon_1 = 0{,}05\%$ and $\varepsilon_2 = 0{,}25\%$. For specimens in ISO 179, data from the pointer's readings were written down after the pendulum impact test and imported into Microsoft Excel for further processing. Descriptive statistics in terms of means and standard deviations were calculated for each group. One-way analysis of variance (ANOVA) was used to analyze intragroup differences. The Mann-Whitney U test was performed after a statistically significant result to confirm the difference between the groups. IBM SPSS Statistics (version 26) was used to analyze the data. The criterion for significance was set to a *p*-value lower than 0.05.

Results

ISO 178 – results of flexural tests

The results of the flexural tests are summarized in Table 7. The sterilization process's effect on the ultimate flexural strength of the specimens was statistically significant in all the groups. For the PLA specimens, sterilization resulted in a statistically significant decrease of the ultimate flexural strength ($p < 0.001$), while for BioMed Clear specimens, it resulted in a statistically significant increase ($p < 0.001$). The flexural modulus increased statistically significantly in all the groups due to the sterilization process ($p < 0.05$). Build orientation was only a statistically significant factor in flexural strength and flexural modulus for the BioMed Clear specimens ($p = 0.009$). Ultimate flexural strength could not be determined for the BioMed Clear specimens because the specimens did not break before the 5% strain. Therefore, flexural strength at 5% strain was used to compare the BioMed Clear specimen groups. In Figure 9 and Figure 10 the results from the flexural tests are visualized in bar charts. Significant differences between pairs are indicated with asterisks.

Table 7.Flexural strengths in MPa, flexural moduli in MPa, and strains in % of the different groups after sterilization with steam in an autoclave.

Group	Non sterilized			Sterilized		
	Ult. flexural strength ± SD [MPa]	**Flexural modulus ± SD [MPa]**	**Strain ± SD [%]**	**Ult. Flexural strength ± SD [MPa]**	**Flexural modulus ± SD [MPa]**	**Strain ± SD [%]**
A1	91.31 ± 0.90	3597.35 ± 114.79	3.74 ± 0.20	60.67 ± 3.46	4021.52 ± 124.60	1.50 ± 0.08
A2	86.37 ± 1.23	3525.16 ± 215.78	4.05 ± 0.05	75.55 ± 2.80	4325.89 ± 258.79	1.67 ± 0.04
A3	97.41 ± 0.80	3614.97 ± 131.22	4.04 ± 0.19	59.82 ± 3.84	4509.64 ± 144.80	1.41 ± 0.10
A4	106.00[a] ± 1.89	3808.35 ± 90.07	6.45 ± 2.89[b]	80.44 ± 3.67	4550.46 ± 323.21	1.71 ± 0.09
A5	56.46[a] ± 2.03	1550.86 ± 76.54	5.51 ± 0.00[b]	71.19[a] ± 2.58	2034.83 ± 36.97	5.19 ± 0.66[b]

A6	67.90[a] ± 1.28	1865.30 ± 70.33	5.00 ± 0.00[b]	82.60[a] ± 2.67	2426.33 ± 163.92	4.92 ± 0.07[b]

[a] flexural strength at 5% strain. For specimens that did not reach 5% strain, maximum flexural strength was used.
[b] Specimens did not break in this group. Therefore this is not the maximum strain rate of the material.

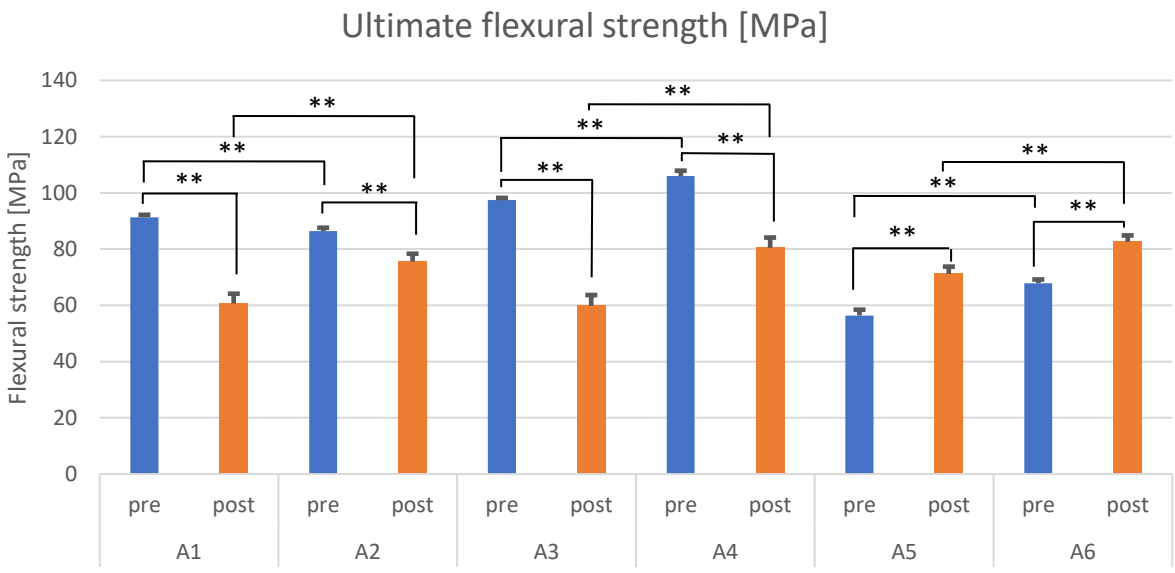

*Figure 9. ISO 178 – Ultimate flexural strengths in MPa for the different groups. 'Pre' indicates the groups of specimens that were not sterilized before flexural tests. 'Post' shows the groups of sterilized specimens. * indicates a p-value less than 0.05 between pairs, and ** indicates a p-value less than 0.01.*

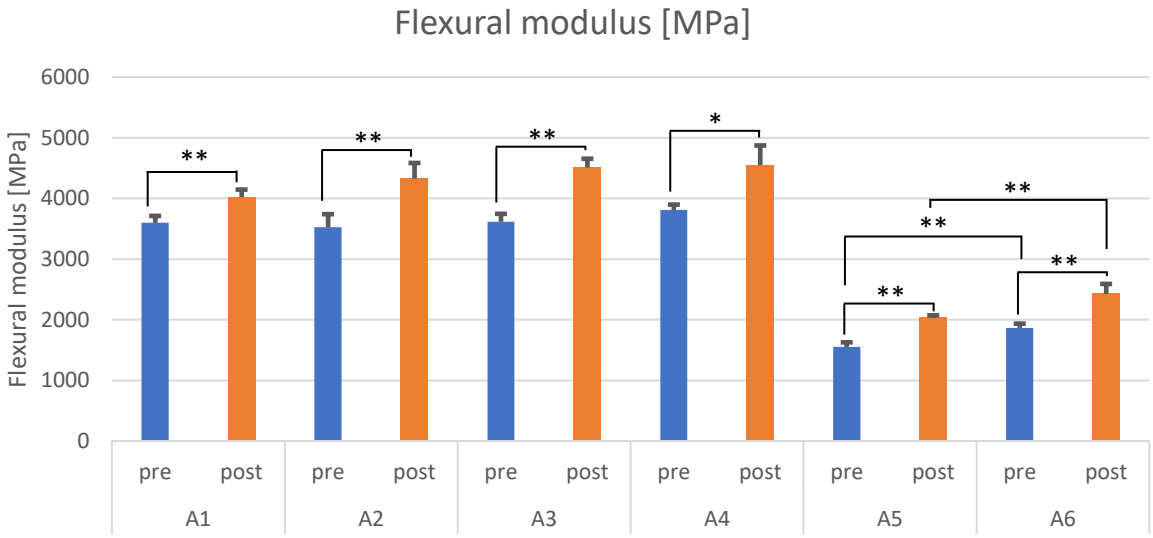

*Figure 10. ISO 178 – Flexural moduli in MPa for the different groups. 'Pre' indicates the groups of specimens that were not sterilized before flexural tests. 'Post' shows the groups of sterilized specimens. * indicates a p-value less than 0.05 between pairs, and ** indicates a p-value less than 0.01.*

The print orientation effect on the BioMed Clear specimens was visual as it resulted in significant warping of specimens printed at a 0° angle. In Figure 11, the top and side view of two BioMed Clear specimens are shown. In both pictures, the left sample was printed at a 45° angle relative to the build platform. Specimens from groups A5 and A6 did not break during the flexural testing and maintained their shape.

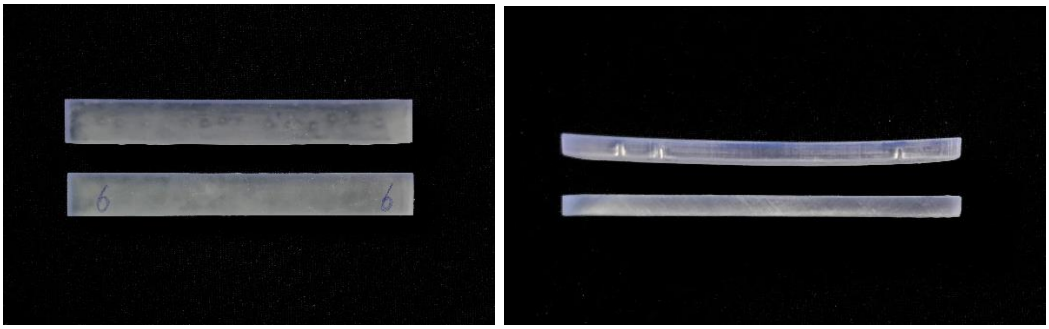

Figure 11. ISO 178 – Biomed clear resin specimens printed at different build orientations. In both pictures, the bottom specimen is printed at a 45 angle relative to the build platform. These specimens showed less deformation in terms of warpage.

ISO 179 – results from Charpy impact tests

The results obtained from the Charpy impact tests are summarized with mean values for each group in Table 8. All 72 specimens showed complete break after impact with the pendulum swing. The sterilization process's effect resulted in a statistically significant decrease of the Charpy impact strength in five groups, namely groups 1-4 and 6. Group 5 did not show a statistically significant difference between the pre- and post-sterilization measurements (p = 0.055). Build orientation did not significantly affect the Charpy impact strength for PLA samples printed with 60% infill (un-sterilized and sterilized) and sterilized PLA samples with 100% infill. The p-values were 0.078, 0.631, and 0.150 respectively. Specimens from BioMed clear resin printed at a 45° angle had a statistically significantly increased notched impact strength than the specimens printed at a 0° angle (p = 0.004 for both unsterilized and sterilized groups). Infill percentage did not have a statistically significant effect on the Charpy impact strength for PLA models. In Figure 12 the results from the Charpy notched impact tests are visualized in a bar chart. Significant differences between pairs are indicated with asterisks.

Table 8. ISO 179 – Results of the Charpy notched impact tests for each group. Values are in kJ/m^2 and are averaged for each group. The standard group indicates groups with unsterilized specimens.

Group	Notched impact strength [kJ/m^2]		
	Standard ± SD	Sterilized ± SD	% change
A1	4.27 ± 0.70	2.88 ± 0.53	-32.5
A2	3.67 ± 0.32	2.91 ± 0.30	-20.8
A3	3.95 ± 0.31	3.02 ± 0.46	-23.5
A4	3.50 ± 0.24	2.66 ± 0.21	-24.0
A5	4.11 ± 0.66	3.41 ± 0.37	-17.1
A6	7.00 ± 1.03	5.50 ± 0.61	-21.5

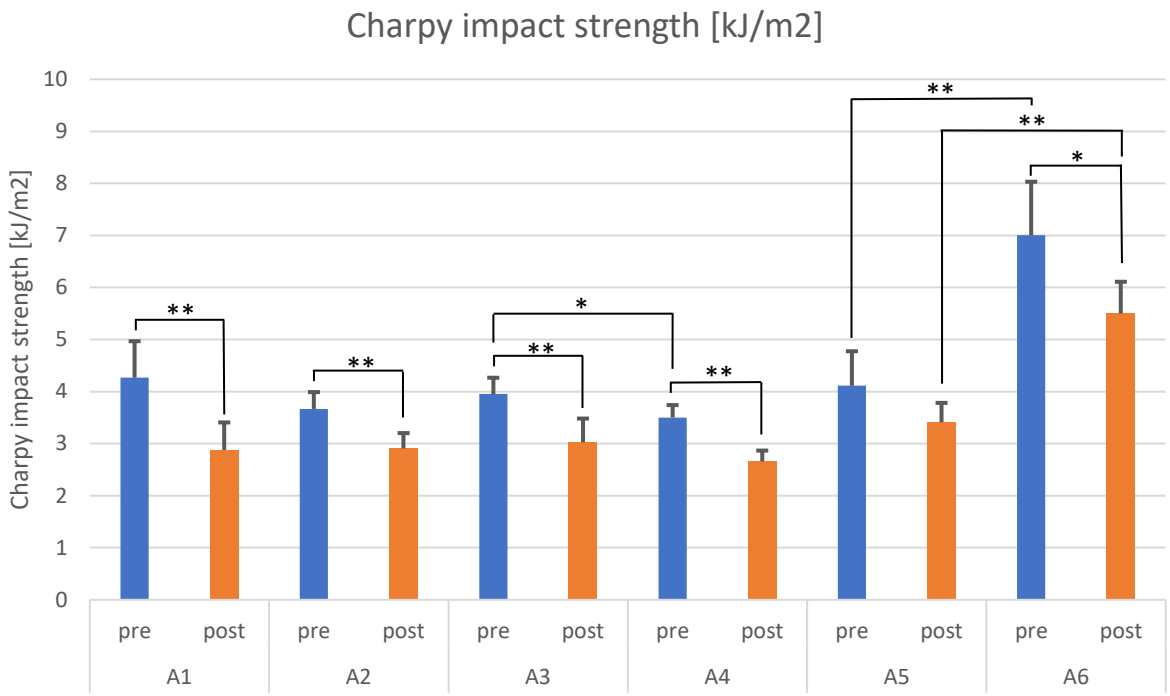

*Figure 12. ISO 179 – Charpy notched impact strength test results in kJ/m² for the different groups. 'Pre' indicates the groups of specimens that were not sterilized before impact tests. 'Post' shows the groups of sterilized specimens. * indicates a p-value less than 0.05 between pairs, and ** indicates a p-value less than 0.01. 13*

ISO 527 – results of tensile tests

The effect of sterilization was visible on the PLA models, as they showed significant deformation compared to the non-sterilized PLA specimens. For the sterilized PLA specimens printed at the 0° orientation angle, 6/10 specimens deformed so much that mechanical testing could not be performed. In Figure 14, the effect of the sterilization process on PLA printed specimens is visualized. In all six of the deformed PLA specimens, the grip areas were inflated by the sterilization process's moisture and heat. Therefore, they could not fit between the grips of the testing machine.

Figure 14. ISO 527 – The effect of the sterilization process on PLA specimens with 60% infill printed in the 0 degrees orientation. The specimen on the left is the sterilized sample in both pictures. The sample on the right is the unsterilized variant.

For the specimens printed in BioMed Clear resin, the post-processing step in terms of washing and curing resulted in significant warping of the 0° printed samples, group A5. Furthermore, the sterilization process resulted in the delamination of the top layer of the specimens in this group, shown in figure 15. As mentioned earlier in the materials and methods section, this effect can be minimized by rotating the specimens at a 45° angle relative to the build platform to limit the surface contact area that the print has with the resin tank during printing. According to Formlabs, the delamination effect can have multiple causes, and one of them is model orientation. An explanation for the delamination of the top layer of the model is the peel forces that the model experiences during printing. After every printed layer, the build platform rises slightly to prepare for the next layer to be printed. The wiper then moves left and right between each layer, which, according to Formlabs, can cause strain along the XY axis and lead to warping (13). Flat surfaces that are orientated parallel to the build platform are especially susceptible to peel forces. It is thought that these peel forces have resulted in the delamination of the model's top layers. The heat of the steam sterilization process has then resulted in the enlarged effect visible in Figure 13.

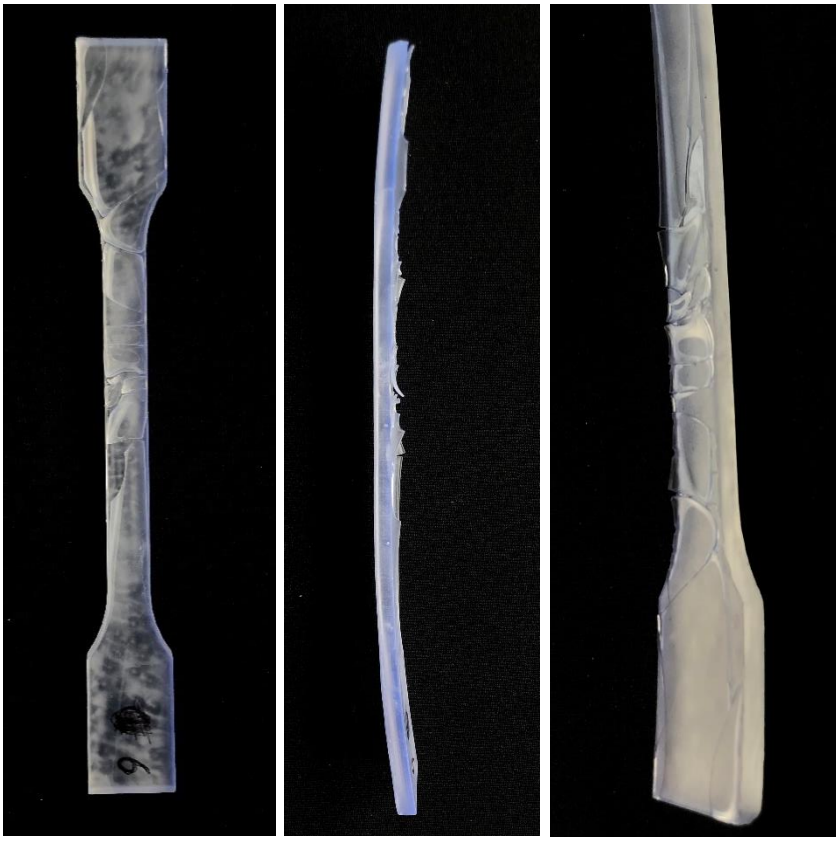

Figure 15. ISO 527 – Biomed Clear resin specimen printed at a 0° angle. On the left: top-view of the specimen. Middle: side-view with significant warping. Right: visual delamination of the top layer of the specimen due to the sterilization process. Delamination only implied for specimens printed at 0°.

In Table 9, the mean mechanical testing values for each group are summarized. Steam sterilization resulted in an overall increase in ultimate tensile strength for group A6 only. However, this increase was not statistically significant (p = 0.117). For groups A1-A5, sterilization resulted in decreases in ultimate tensile strength, where only for group A3 the effect was statistically not significant (p = 0.143), as shown in Figure 14. This can be explained as for the sterilized samples in group A3 only one specimen could be tested. The tensile modulus increased due to sterilization in group A2 (p = 0.009), group A4 (p = 0.028), and group A6 (p = 0.175) (Figure 15). For group A1, group A3, and group A5 the effect of steam sterilization resulted in decreases in tensile modulus that were statistically not significant for any of the groups, i.e., p = 0.655, p = 0.380, and p = 0.076, respectively. The build orientation had a statistically significant effect on the ultimate tensile strength and tensile modulus in all

groups except for the sterilized PLA groups with 100% infill (p = 0.143). However, in this group, 4/10 specimens could not be tested due to the specimen's deformation by the sterilization process. The infill percentage effect was significantly different for all the A groups containing PLA specimens, except for sterilized PLA specimens printed at 0 degrees (p = 0.180) as 6/10 specimens could not be tested. In Figure 16 and Figure 17 the results from the tensile tests are visualized in bar charts. Significant differences between pairs are indicated with asterisks.

Table 9. ISO 527 – Results of the tensile tests for each group. Values are in MPa and are averaged for each group.

Group	Non sterilized			Sterilized		
	Ult. Tensile strength [MPa]	Tensile Modulus [MPa]	Elong. [%]	Ult. Tensile Strength [MPa]	Tensile Modulus [MPa]	Elong. [%]
A1	34.83 ± 1.81	2348.22 ± 102.60	2.26 ± 0.15	7.83 ± 3.45	2194.79 ± 375.32	0.40 ± 0.07
A2	36.62 ± 0.64	2759.82 ± 27.92	1.72 ± 0.03	17.61 ± 4.84	3156.54 ± 180.61	0.63 ± 0.13
A3	50.45 ± 1.27	3234.24 ± 42.98	2.85 ± 0.42	13.20 ± 0.00	3213.66 ± 0.00	0.44 ± 0.00
A4	59.27 ± 1.85	3512.25 ± 111.55	2.30 ± 0.31	31.39 ± 3.73	4058.42 ± 365.38	0.85 ± 0.05
A5	44.66 ± 0.64	1895.71 ± 45.08	6.94 ± 1.28	25.53 ± 10.18	1786.36 ± 116.77	1.30 ± 0.49
A6	46.76 ± 0.67	2069.58 ± 36.58	8.90 ± 4.76	47.35 ± 0.92	2098.16 ± 11.48	4.29 ± 0.50

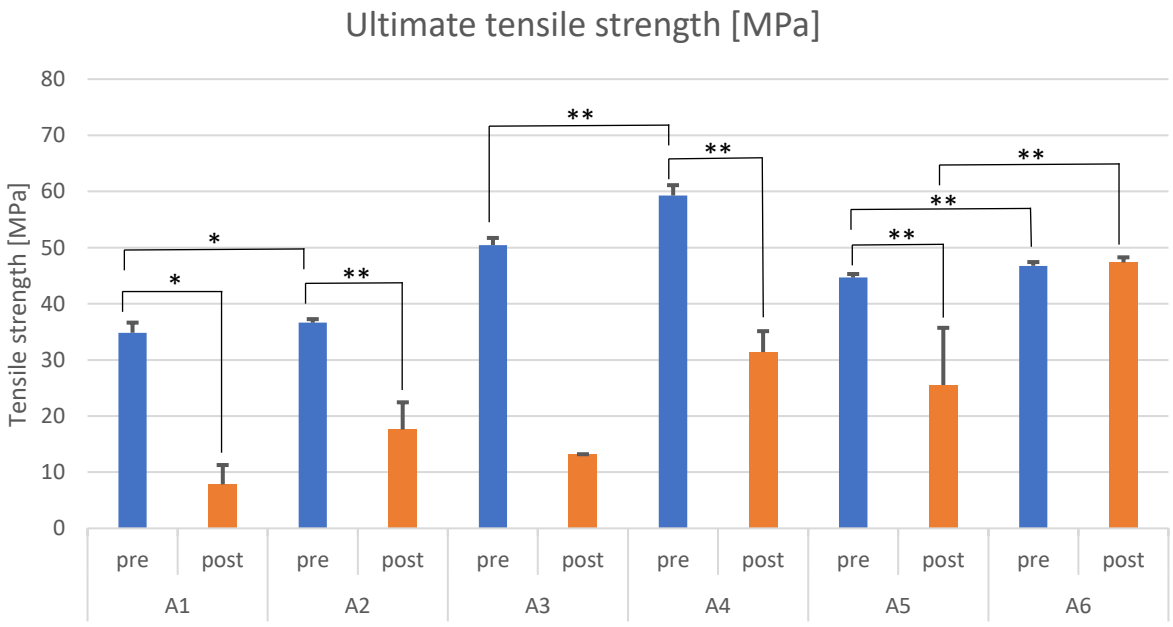

*Figure 16. ISO 527 – Ultimate tensile strength in MPa for the different groups. 'Pre' indicates groups of specimens that were not sterilized before impact tests. 'Post' shows groups with sterilized specimens. * indicates a p-value less than 0.05 between pairs, and ** indicates a p-value less than 0.01.*

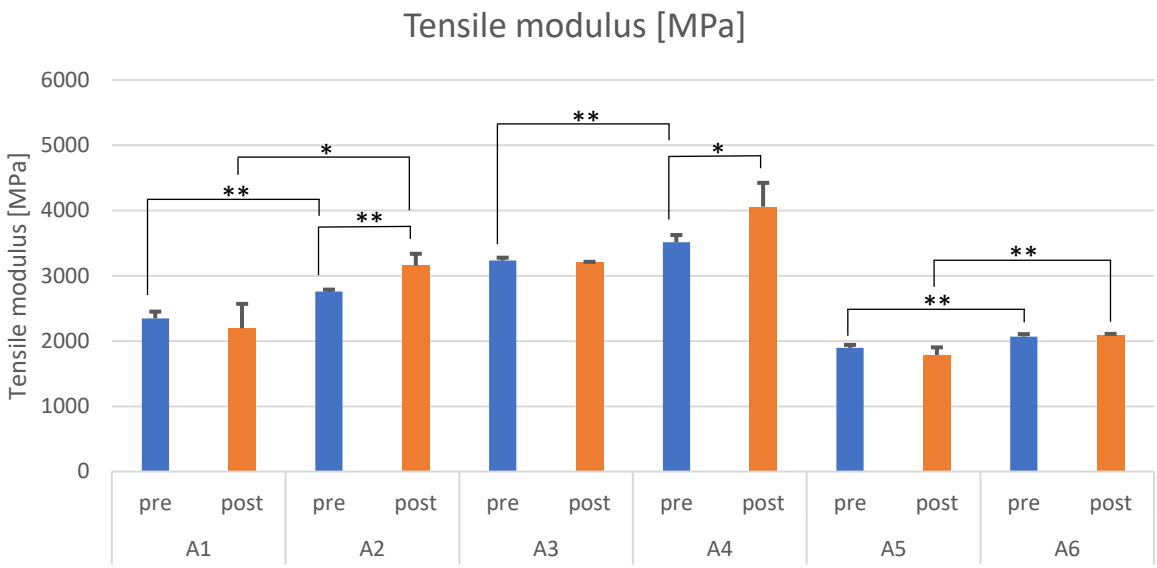

*Figure 17. ISO 527 – Tensile modulus in MPa for the different groups. 'Pre' indicates groups of specimens that were not sterilized before impact tests. 'Post' shows groups with sterilized specimens. * indicates a p-value less than 0.05 between pairs, and ** indicates a p-value less than 0.01*

Part B – Dimensional tests

Materials & methods

The steam sterilization process's effect on the dimensional accuracy of 3D printed BioMed Clear resin models was investigated. A 3D model of a surgical cutting guide for a distal radius correction osteotomy (Figure 18) was used to print five samples in Biomed Clear V1 resin (Formlabs, Somerville, MA, USA) with the Form 2 printer (Formlabs, Somerville, MA, USA). The models were printed with a 0.1 mm layer thickness and orientated at a 45° angle relative to the build platform. Post-processing of the samples was performed according to Formlabs' instructions for printing medical grade resins. This implied: rinsing in ≥ 99.85% Isopropyl Alcohol (IPA) (JAGRO Solutions B.V., http://deoplosmiddelspecialist.nl) for 15 minutes; drying at room temperature for 30 minutes; post-cure at 60°C for 60 minutes in the Form Cure (Formlabs, Somerville, MA, USA); removal of support material with fine cutting pliers. According to the hospital's protocol for sterile medical devices, all five specimens were sterilized with steam in an autoclave at 134°C for 3.5 minutes. The sterilization procedure was previously described in the materials and methods section for mechanical testing (Part A) under the 'Sterilization method.'

Figure 18. On the right: the digital 3D model of the surgical guide that is used for dimensional testing. When this thesis is opened in Word, one can view the model from different angles as it is implemented as a 3D model. On the right: 3D printed result in BioMed Clear resin.

Digitization of the 3D Printed Models

The models were scanned with a TRIOS 3 Intraoral Scanner (3Shape, Copenhagen, Denmark) before and after the sterilization process (Figure 19). The supplied manufacturer's specifications for the scanner included trueness (accuracy) of 6.9 (± 0.9) μm and a precision (consistency) of 4.5 (± 0.9) μm. The Implant Planning Scanning method of the scanner was used to scan the models. Helling 3D scanning spray was applied in the small crevices as the 3D scanner was unable to scan these surfaces without using the scanning spray. The scanning spray was applied by first fully covering the models. After sufficient drying time, the outer surface of the models was cleaned with water and IPA. Therefore, only the small crevices contained 3D scanning spray on the surface. The resulting scanned models were exported as Standard Tessellation Language (STL) files. The scanner was calibrated every day it was used by the dental practitioner.

Figure 19. Left: 3Shape Trios Intraoral Scanner. The scanner can be seen in the holder next to the touchscreen. Right: Helling 3D scanning spray that was used for the small crevices in the 3D printed model.

Accuracy Analysis

The STL files of the model pre- and post-sterilization were imported into the 3D slicer software (3DSlicer, http://www.slicer.org). Firstly, the post-sterilization STL model was superimposed over the pre-sterilization reference model by manual alignment using translational and rotational adjustments in 3D Slicer, as can be seen in Figure 20. Then, a surface registration module in Slicer (CMFreg, http://www.nitrc.org) was used to match the entire meshes of both STL models using the Iterative Closest Point Algorithm. The registration module uses rigid, similarity, or affine transformations to register the two models and does not require the two models to have the same number of points (14). After the models were superimposed, a part comparison analysis was applied using the model-to-model distance module in Slicer (3DMeshMetric, http://www.nitrc.org). This point-based analysis algorithm (signed closest-point) recorded the positive or negative deviations for each point between the two groups (pre- and post-sterilization) with the pre-sterilization model as a reference.

The resulting Visualization Toolkit (VTK) file contained the relative distances in millimeters between the pre- and post-sterilization models. A distance heat map was created to visualize whether one model's surface was located inside or outside the other model. This was done using the Shape Population Viewer module in Slicer (ShapePopulationViewer, http://www.nitrc.org). ParaView software (http://paraview.org, Kitware Inc., New York, USA) was used to extract the point-to-point distances between the pre- and post-sterilization models. Data was then analyzed in Matlab R2020b. The point-to-point mean distance and the Root Mean Square (RMS) value between the pre- and post-sterilization STL files were calculated for every model. The RMS value provides information about the mean value of errors by comparing two data groups (pre- and post-sterilization) with an identical coordinate system. A high RMS value indicates a large error, i.e., a large difference between the measured data to the reference data. The RMS value is used to measure the similarity between two datasets after optimal superimposing of both models. The equation used to calculate the RMS value between the two datasets is:

$$RMS = \sqrt{\sum_{i=1}^{n} \frac{(x_{pre} - x_{post})^2}{n}}$$

where n is the number of measurement points, x_{pre} is the data point for the pre-sterilization point, and x_{post} is the data point for the post-sterilization model. For every model, more than 40.000 measurement points are compared.

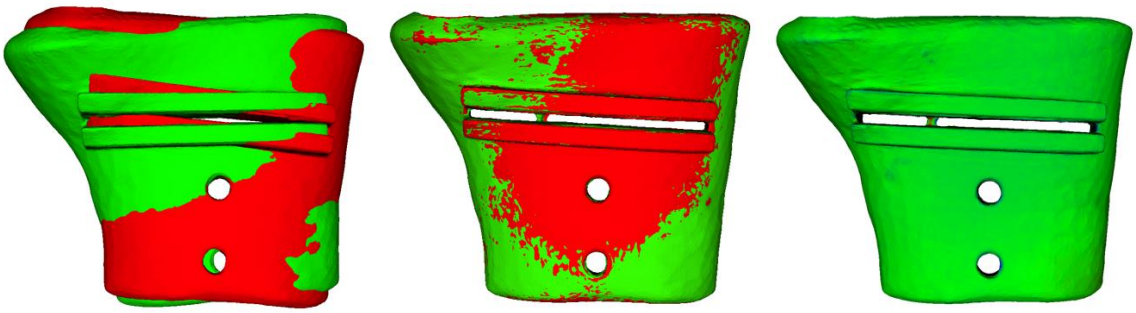

Figure 20. Left: unaligned STL models visualized with the pre-sterilization file in red and the post-sterilization file in green. Middle: models are aligned based on surface registration. Right: resulting model-to-model distance model between pre- and post-sterilization STL files.

Statistical analysis

The data were collected and further analyzed in Matlab version R2020b. Deviations in dimensional accuracy between the model pre- and post-sterilization were quantified using the descriptive statistics (means ± standard deviation) for each model. Furthermore, the RMS value and the minimum and maximum deviations between corresponding points were mentioned. Each model's data were represented as mean, standard deviation, median, and first and third quartile ranges in Box and Whisker plots.

Results

In Figure 21, the Box and Whisker plots for each model are visualized. The red center line indicates the median, and the bottom and top edges of the box indicate the 25th and 75th percentiles, q_1 and q_3, respectively. The whiskers extend to the most extreme data points not considered outliers. Outliers could be visualized. However, in this study, it is chosen not to show them for a better visual understanding. A data point is considered an outlier if its value is more significant than q_3 + 1.5 (q_3-q_1) or less than q_1 - 1.5 (q_3-q_1).

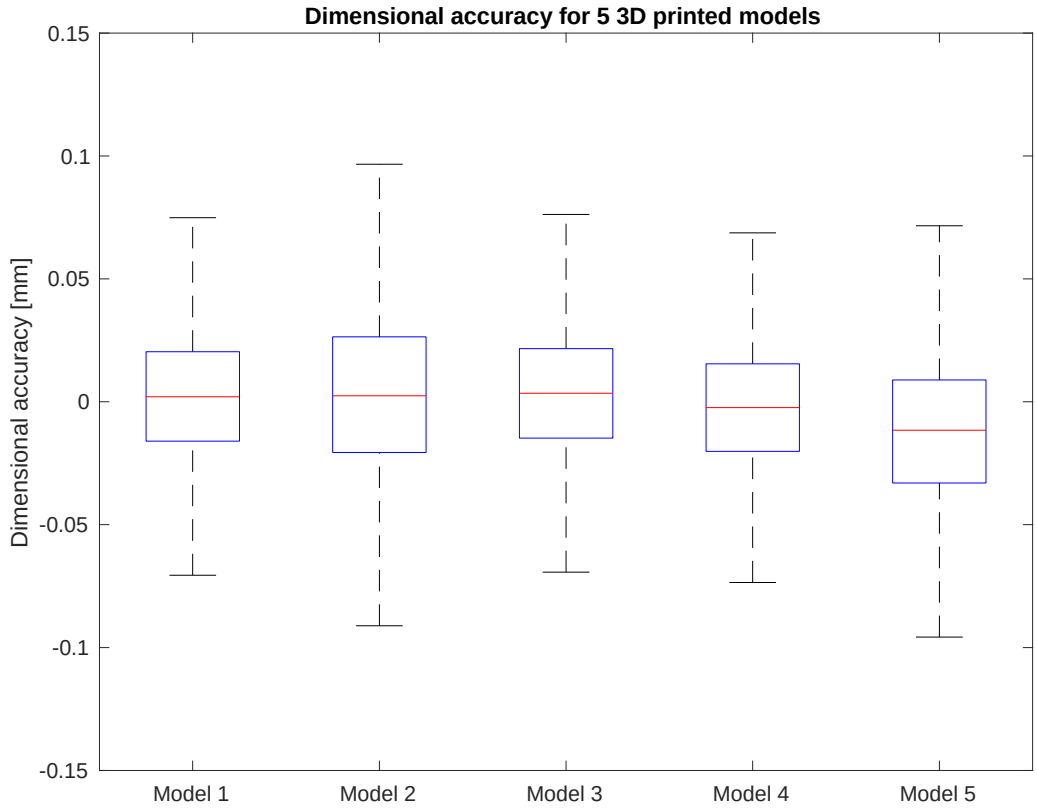

Figure 21. Boxplots for each model between the pre- and post-sterilization measurements. In each box, the central mark indicates the median, and the bottom and top edges of the box indicate the 25th and 75th percentiles, respectively. The whiskers extend to the most extreme data points not considered outliers.

Table 10 summarizes the mean difference values for each model between the pre- and post-sterilization measurements. The standard deviation and the RMS values are closely related in all five of the models. This is because the standard deviation is calculated with the use of the mean value of the measurements. For a set of measurements, the closer the mean value to zero, the closer the RMS value to the standard deviation. The equation for the standard deviation is as follows:

$$\sigma = \sqrt{\frac{\sum(x_i - \mu)^2}{N}}$$

where σ is the standard deviation, N is the number of data points for the model, x_i is the relative distance between two corresponding data points, and μ is the mean deviation of all points.

Table 10. Summary of dimensional difference values for the 3D models between the pre- and post-sterilization STL files.

Model	Mean [μm]	Standard deviation [μm]	RMS [μm]	Minimum [mm]	Maximum [mm]
B1	2.32	33.00	33.08	-0.25	0.22
B2	2.71	40.10	40.19	-0.40	0.30
B3	6.06	33.71	34.25	-0.19	0.36
B4	-0.96	36.56	36.57	-0.71	0.35
B5	-11.05	33.07	34.87	-0.18	0.13

The distance heat map of the models is provided in Figure 21. In the distance heat map, the blue areas indicate the negative deviations, whereas the red areas correspond to positive deviations. The green areas indicate a high degree of agreement between the pre- and post-sterilization STL model, which accounted for the model's largest part. Compared to the model's outer surface, the small crevices usually showed larger dimensional deviations. These were more difficult to scan with the intraoral 3D scanner, even with laser scanning spray. The histograms in Figure 21 visualize the frequency at which a given deviation occurs between data points.

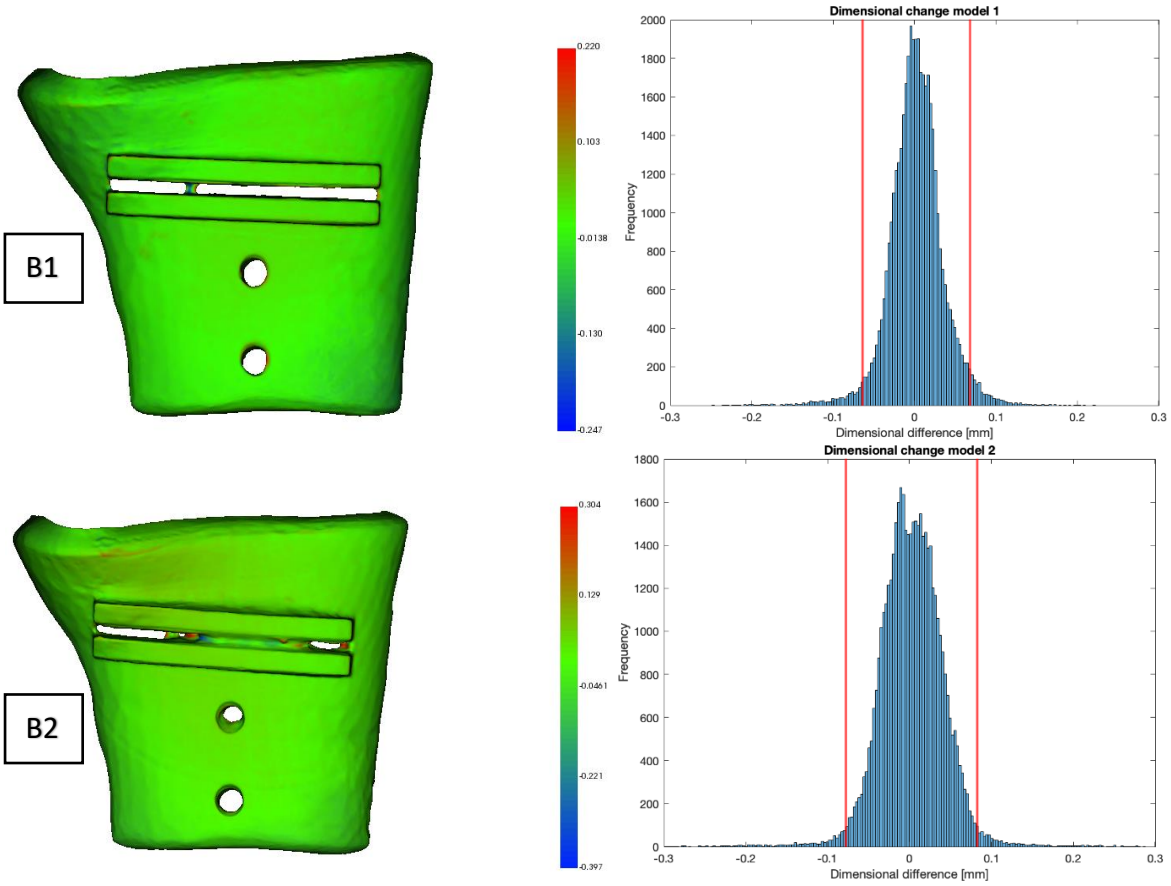

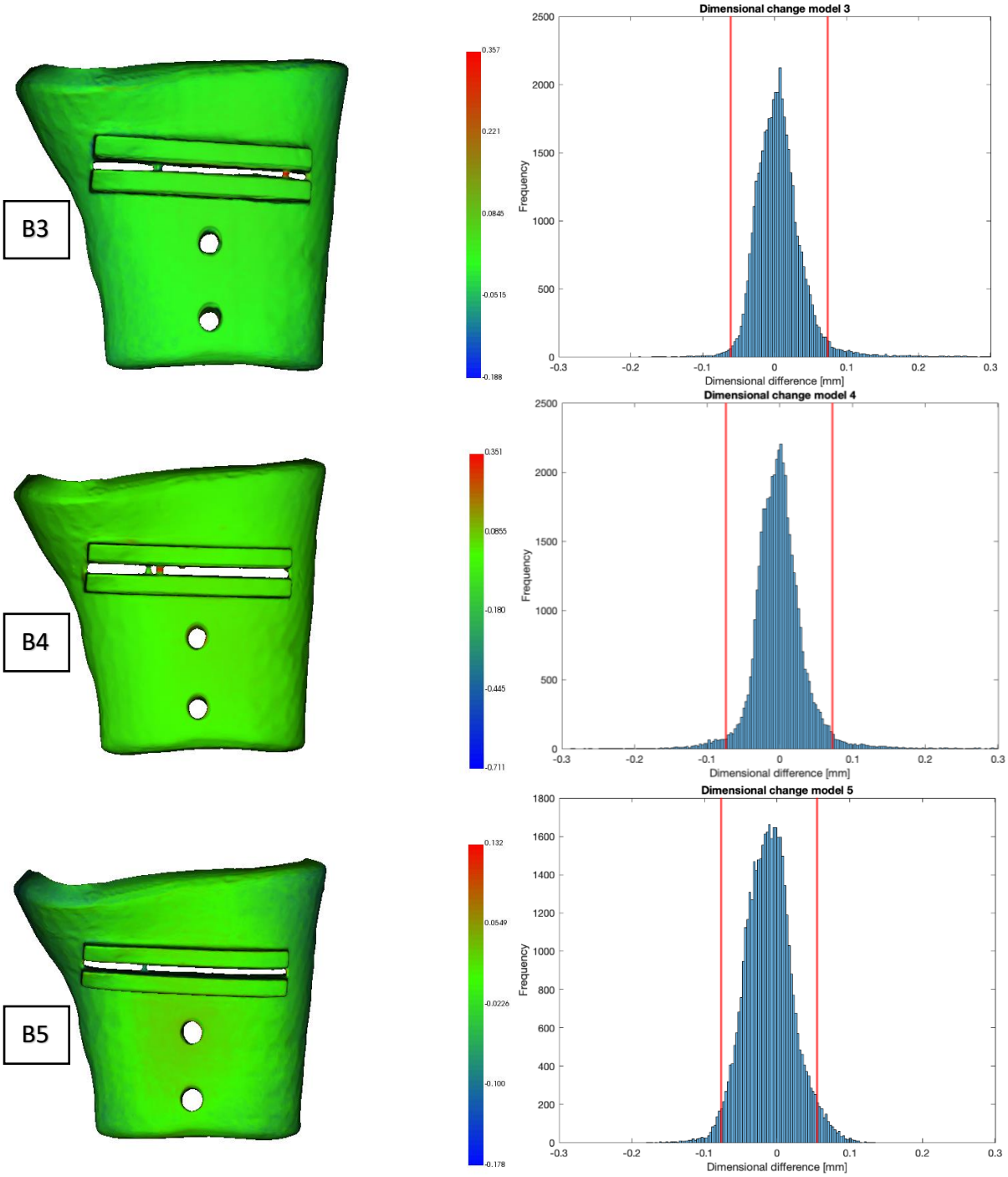

Figure 22. Distance heat map per model combined with a histogram containing dimensional differences between the pre- and post-sterilization STL models. The red lines in the histograms indicate the upper and lower bounds of the 95% confidence intervals.

Part C – Sterility testing

Materials & Methods

Equipment and materials

To verify that the Elisabeth Two-Cities hospital's sterilization process could deliver sterile medical devices for operational procedures, sterility testing was performed for five different workflows of in-house fabricated patient-specific surgical guides. The five different workflows were divided into five groups, and each group contained five specimens manufactured with in-house available 3D printers. Specimens in group C1-C4 were printed with the Form 2 printer (Formlabs Inc., Somerville, MA, USA) in Biomed Clear resin (Formlabs Inc., Somerville, MA, USA). PreForm software v 3.8.1 (Formlabs Inc., Somerville, MA, United States) was used to prepare and orientate the specimens on the build platform. Specimens were printed with a layer thickness of 100 microns, and supports were generated with the auto-generation feature. The Form Wash (Formlabs Inc., Somerville, MA, USA) and Form Cure (Formlabs Inc., Somerville, MA, USA) were used to post-process the specimens in these groups directly after the printing procedure was finished. For specimens in group C5, the Ultimaker S5 printer (Ultimaker B.V., Utrecht, The Netherlands) was used to print specimens in Pearl-White PLA (Ultimaker B.V., Utrecht, The Netherlands). Polyvinyl alcohol (PVA) was used as a supporting structure. Group C5 was added to the sterility testing procedure for comparison purposes. In Table 11, the workflows of the five groups are summarized.

Table 11. A brief overview of the workflow from print to sterility test for the different groups.

Group	Description	Workflow
C1	Form 2 print process	Form 2 → sterility test
C2	Effect of steam sterilization	Form 2 → sterilization → sterility test
C3	S. Aureus contamination	Form 2 → S. Aureus contamination → sterilization → sterility test
C4	Sterile storage (4 weeks)	Form 2 → sterilization → 4 weeks of sterile storage → sterility test
C5	Ultimaker S5 print process	Ultimaker S5 → sterility test

Design and 3D printing of specimens

Specimen design was based on a patient-specific surgical cutting guide for a distal radius correction osteotomy. In Figure 23, five specimens are shown on a build platform in the PreForm software with supporting structures in the grey color.

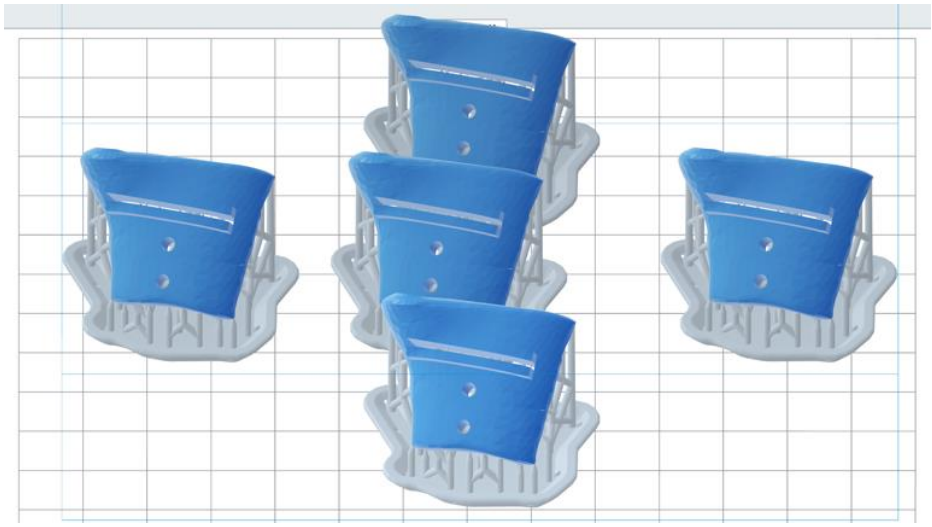

Figure 23. Five models are visualized on the build plate in the PreForm software. The support structure is colored grey and is printed with the same material.

Post-processing of the specimens

A total of 20 specimens were printed from Biomed Clear resin with the Form 2 printer. After the printing process, specimens were removed from the build plate and washed in the Form Wash in 99% Isopropyl Alcohol (IPA) for 15 minutes to remove the uncured resin. Subsequently, models were air-dried at room temperature for 30 minutes to allow the solvent to evaporate from the surface of the specimen fully. After the specimens were dried, they were placed in the Form Cure at 60 °C for 60 minutes to achieve optimal material properties. Support structures were removed after the Form Cure process with the use of removal tools. The specimens were then disinfected in fresh 99% IPA for 5 minutes.

The five specimens in group C5 were printed with the Ultimaker S5 from Pearl-White PLA. After the printing process was finished, 3/5 samples were removed from the build platform with sterile gloves, and the supporting structure was removed with disinfected (99% IPA, 5 min) removal tools. Samples were then stored in BOP paper/film pouches before their transport to the Medical Microbiology Department (MMD). The remaining 2/5 specimens were post-processed according to the standard procedure for the removal of PVA support structures. This implied gross removal of the support structure with removal tools, followed by dissolving the specimens in water until the PVA structure was dissolved. The specimens were then also stored in BOP paper/film pouches for their transport to the MMD.

Workflow from printing to sterility testing

Specimens in Group C1 were tested on bacterial contamination directly after the Form 2 printing process. After the post-processing step was finished, specimens were placed in BOP paper/film pouches with sterile gloves to minimize the chance of contamination. The separately packed specimens were then transported to the MMD in a plastic box for sterility tests.

Specimens in Group C2 were sterilized according to the hospital's workflow for the sterilization of medical devices with steam at 134 °C for 3.5 minutes. The sterilization method is previously described in the mechanical tests' materials and methods section (Part A). Directly after the sterilization process, the specimens were tested on bacterial contamination at the MMD.

Specimens in Group C3 were consciously contaminated at the MMD with *Staphylococcus Aureus* (S. aureus) before being sterilized with steam. After the sterilization process, the models were tested on bacterial contamination once again.

Group C4 contained specimens that were stored for four weeks in a sterile storage room after being sterilized with steam. After four weeks of sterile storage, the models were tested on bacterial contamination at the MMD.

Specimens in Group C5 were tested on bacterial contamination directly after the Ultimaker S5 printing process. After removing the support structures, models were placed in BOP paper/film pouches and transported to the MMD for sterility testing.

Medical Microbiology Department protocol

At the MMD, sterile tweezers were used to place the specimens separately in Brain Heart Infusion (BHI) broth in a laminar flow cabinet. Samples were stored at 37 °C for 14 days. After 14 days, if the broth showed bacterial contamination by turning cloudy, the broth was placed on agar plates in a laminar flow cabinet with an inoculation loop by streaking. Chocolate agar, blood agar, and TGEA agar (tryptone glucose yeast extract agar) were used as a growth medium to culture microorganisms. The agar plates were incubated at 37 °C for five days. After five days, the agar plates were visually examined for bacterial growth, and the number of colonies was noted.

The agar plate's bacterial growth was analyzed via Matrix-Assisted Laser Desorption Ionization Time-Of-Flight Mass Spectrometry (MALDI-TOF MS). This technique uses a matrix solution to overlay microbial samples deposited on a target plate (15, 16). The target plate is then placed in the instrument where short laser pulses ionize the sample, thereby creating gas-phase ions. These ions are accelerated in a vacuum through an electrical field. The time it takes for a particle to reach the detector is called time-of-flight and depends on its charge and mass. The resulting *m/z* ratio can be calculated by dividing the atomic mass *(m)* by the ion's charge number (z). After a mass spectrometer has detected all the particles, a spectral fingerprint that is unique for the organism is produced. In Figure 24, the principle of MALDI-TOF MS is schematically visualized (17).

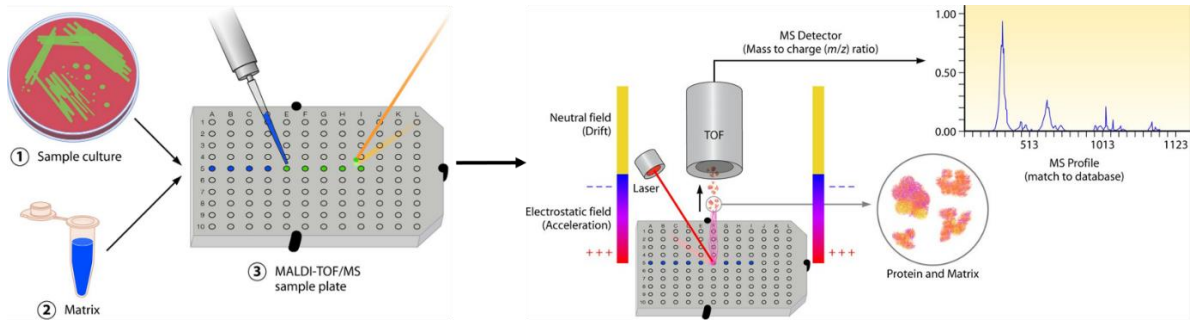

Figure 24. The process of MALDI TOF mass spectrometry (17)

The organism can then be identified using software that compares its spectral profile with a reference database. Generally, the spectra obtained from the target samples are not entirely identical to the database's references. Therefore, a 'score value' is assigned to each match between the target sample spectra and the reference spectra. For the tests performed in this experiment, a score value of greater than or equal to 2.000 was used for the cut-off identification of bacteria. In case the score value was between 1.700 and 2.000, the term ''species' was used in combination with the bacteria's genus hierarchy. When the score value was lower than 1.700, no reliable identification could be performed.

Results

In Table 12, the results in terms of contaminated specimens per group are summarized. For specimens that were tested directly after the printing process, 9/10 specimens were contaminated with bacteria, of which all of them are likely to originate from the human skin flora. For the groups that contained sterilized samples before their sterility testing, 1/15 samples tested positive on bacterial contamination.

Table 12. Summary of the number of specimens contaminated with bacteria within each group.

Group	Description	Specimens with bacterial growth
C1	Form 2 print process	4/5
C2	Sterilization	0/5
C3	S. Aureus contamination	1/5
C4	Sterile storage (4 weeks)	0/5
C5	Ultimaker S5 print process	5/5

Group C1 – Form 2 print process

Table 13 shows the results of the MALDI TOF MS measurements on the specimens' bacterial growth for group 1. Results show that 4/5 samples were still contaminated with bacterial growth after the printing process. All of the four microorganisms present on the specimens are part of the human skin flora.

Table 13. Results from the MALDI-TOF MS testing of specimens in group C1, after the Form 2 printing process.

Specimen	Bacteria	Shape	Habitat	Gram stain	Metabolism	Pathogenicity
1	-	-	-	-	-	-
2	***Staphylococcus capitis***	Coccus (Spherical)	Human skin flora	Positive	Coagulase-negative species (CoNS), Aerobe	Prosthetic valve endocarditis
3	***Corynebacterium species***	Bacilli (rod)	Human skin flora	Positive	Aerobe	Usually not pathogenic
4	***Cutibacterium acnes***	Bacilli (rod)	Human skin flora, gastrointestinal tract	Positive	Aerotolerant Anaerobe	Acne, blepharitis, endophthalmitis
5	***Micrococcus luteus***	Coccus (Spherical)	Human skin flora, upper respiratory tract, soil, water, air	Positive	Aerobe	Usually not pathogenic

Group C2-C4

For specimens in group C2 and C4, none of the specimens were contaminated with bacteria after the sterilization procedure. For the specimens in group C3, only one specimen was contaminated with a *cutibacterium species,* summarized in Table 14.

Table 14. Results from the MALDI-TOF MS testing of groups C2-C4. One specimen in group C3 was contaminated.

Group & specimen number	Bacteria	Shape	Habitat	Gram staining	Metabolism	Pathogenicity
Group C3 5	***Cutibacterium species***	Bacilli (rod)	Human skin flora	Positive	Anaerobe	Usually not pathogenic

Group C5 – Ultimaker S5 print process

Specimens tested on sterility after the 3D printing process with the Ultimaker S5 all tested positive on bacterial contamination. For specimens 1-3 that were processed with sterile gloves, the bacteria present appear to originate from the human skin flora. Specimens 4 and 5 were processed in water and contained bacteria usually present on the human skin flora or in water and soil. The results of bacterial identification by MALDI-TOF MS are summarized in Table 15.

Table 15. Results from the MALDI-TOF MS testing of group C5, after the Ultimaker S5 printing process.

Specimen	Bacteria	Shape	Habitat	Gram staining	Metabolism	Pathogenicity
1	***Bacillus species***	Bacilli (rod)	Human skin flora, large intestine	Positive	Aerobe and Anaerobe	Usually not pathogenic
2	***Dermabacter hominis***	Cocci (spherical) or Bacilli (rod)	Human skin flora	Positive	Aerobe and Anaerobe	Usually not pathogenic
3	***Corynebacterium tuberculostearicum***	Bacilli (rod)	Human skin flora, mucosae	Positive	Aerobe	Usually not pathogenic
	Micrococcus luteus	Cocci (Spherical)	Human skin flora, upper respiratory tract, soil, water, air	Positive	Aerobe	Usually not pathogenic
4	***Staphylococcus species***	Cocci (spherical)	Human skin flora, mucosae	Positive	Aerobe and Anaerobe	Usually not pathogenic, Coagulase-positive staphylococci are typically more virulent
5	***Staphylococcus capitis***	Coccus (Spherical)	Human skin flora	Positive	Coagulase-negative species (CoNS), Aerobe	Prosthetic valve endocarditis
	Sphingomonas paucimobilis	Bacilli (rod)	Water, soil	Negative	Aerobe	Usually not pathogenic, nosocomial infections

Discussion

Mechanical properties

The goal of this research was to determine whether the in-house available Form 2 3D printer would be suitable for the production of patient-specific surgical guides.

In Part A of the research, the effect of the in-house steam sterilization method on the mechanical properties of BioMed Clear resin and Pearl-White PLA specimens was investigated. Three different mechanical tests were performed: tensile, flexural, and Charpy notched impact tests. From these tests, lessons were learned that steam sterilization could improve the tensile and flexural properties of BioMed Clear resin specimens. A possible explanation for the increased mechanical properties is the annealing effect of the sterilization process. Annealing can be defined as a process where a material undergoes a heat treatment to a certain temperature, is kept there for a definite time, and is then cooled to room temperature in order to alter the material properties (18). The annealing process increases the material's crystallinity and redistributes the stress within the printed part (19, 20). The amount of crystallinity, in turn, determines the performance of the material, improving stiffness, strength, heat deflection temperature, and chemical resistance. However, as the material becomes more robust in terms of mechanical properties due to annealing, a result is that it is also likely to become more brittle. Looking at the Charpy impact test results, all the groups showed decreases in impact energy after sterilization, which underlines the brittleness of the material. The increased brittleness of polymers after annealing or periodic heating was also confirmed by Abhari et al., who investigated the effect of annealing on electrospun polymer filaments (21). They also concluded that annealing at low temperatures might be more useful as a method to tailor degradation rates for electrospun polymers than to improve mechanical properties.

Sterilized PLA specimens showed large deformations, as illustrated in Figure 12. Most of the deformations occurred for specimens printed at the 0° angle rather than at the 90° angle. At first, it was thought that a possible explanation for the deformation of some sterilized specimens in group A1 and A3 is the 1 mm wall thickness print setting that was used. The 0° orientated specimens had a relatively higher ratio of infill pattern area/ total printed cross-section compared to specimens printed at a 90° angle. As the height and width of the specimens at the gripping positions were 4 mm and 20 mm, respectively, specimens printed at a 90° angle had 50% (2 mm/4 mm) of the cross-section left for infill printing. For specimens printed at 0°, this ratio was 90% (18 mm/ 20 mm). Therefore, it was thought that specimens printed at a 0° angle had relatively more entrapped air inside. However, this statement is inaccurate since specimens printed in both directions have precisely the same infill volume ratio divided by total specimen volume. Therefore, a more realistic and obvious explanation for the difference in deformation due to the sterilization process is the difference in print orientation. For example, specimens both in group A1 and in group A2 had entrapped air inside due to the infill pattern. However, for one group, the sterilization process's heat resulted in deformation of the gripping positions due to the expansion force of the heated and entrapped air. This trapped air was warmed by the steam sterilization process and expanded, resulting in the deformation of the specimens' grip areas. Future studies could investigate whether the expansion of the gripping regions also occurs when different infill geometries are used.

To determine whether BioMed Clear resin is a suitable material for producing patient-specific surgical guides, the 3D print material can be compared to the current gold standard, Polyamide 12. As the mechanical tests in this thesis were performed according to ISO standards for mechanical testing of plastics, the results give a good indication of how the material will perform compared to PA12. The initial goal was also to perform the mechanical tests on PA12 printed specimens; however, this was not possible. Mechanical property values of PA12 specimens were therefore derived from a table provided by Materialise (Materialise, Leuven, Belgium). In Table 16, the mechanical properties of Polyamide 12 are summarized, provided by a manufacturer of patient-specific surgical guides (Materialise, Leuven, Belgium) (22). Values for PA12 were derived from ISO 178, ISO 179, and ISO 527 standards. Next to

the PA12 values, material property data of BioMed Clear are provided by the manufacturer (Formlabs Inc., Somerville, MA, USA) (23). These values were derived using the following American Society for Testing and Materials (ASTM) standards: ASTM D638-10 (Type IV) for tensile properties and ASTM D790-15 (Method B) for flexural properties. For BioMed Clear resin specimens, the measured values from group A6 were used as the specimens used for these tests were printed in the recommended print orientation.

Table 16. A summary of the mechanical material properties of Polyamide 12 and BioMed Clear. The first two columns with values are derived from the manufacturer's technical datasheet. The two columns on the right are values from the mechanical tests performed in this thesis.

	Polyamide 12	**BioMed Clear**	**Measured**	
			Un-sterilized	**Sterilized**
Standard used	**ISO**	**ASTM**	**ISO**	**ISO**
Density (g/cm^3)	0.95 ± 0.03	1.09 [b]	/	/
Tensile Strength (MPa)	48 ± 3	52	46.76	47.35
Tensile Modulus (MPa)	1650	2080	2069.6	2098.2
Flexural strength (MPa)	41	84	67.9 [a]	82.6 [a]
Elongation at break (%)	20 ± 5	12	8.9	4.3
Flexural modulus (MPa)	1500	2300	1865.30	2426.33
Charpy – Impact strength (kJ/m^2)	53 ± 3.8	/	/	/
Charpy – Notched impact strength (kJ/m^2)	4.8 ± 0.3	/	7.00	5.50
Heat deflection temperature	86 °C	67 °C	/	/

[a] *flexural strength at 5% strain. For specimens that did not reach 5% strain, maximum flexural strength was used.*
[b] *technical data of the resin provided by the manufacturer.*

The technical data from PA12 should be compared to the unsterilized BioMed Clear specimens as PA12 technical data provided by the manufacturer was derived from the tests with unsterilized specimens. From Table 17, it becomes clear that, according to the tests performed in this thesis, BioMed Clear specimens have a higher tensile modulus, flexural strength, flexural modulus, and Charpy notched impact strength. This indicates that BioMed Clear resin is a stronger and stiffer material compared to PA12, as it will deform less under a given load. The tensile strength is comparable between the two materials. However, PA12 specimens seem to elongate more when under tension. This can be explained as the material is more flexible. The stiffness of a material can be of great added value for the production of patient-specific surgical guides. The goal of such a surgical guide is to provide a predefined osteotomy path during surgery and to facilitate an accurate translation of the desired surgical treatment plan to reality (24). In case the material of the surgical guide is stiff, the forces applied on the guide by the surgeon are less likely to result in deformation of the guide and thus a deviation from the predefined osteotomy path. Therefore, a stiffer guide is more likely to fulfill the needs of translating the predefined osteotomy path to reality compared to a more flexural guide.

Dimensional properties

In part B of this thesis, the effect of in-house steam sterilization on BioMed Clear printed specimens was investigated. Specimens were scanned with a 3D scanner before and after the sterilization process. At first, the results from the 3D scanner were not sufficient as the scanner was unable to scan the small crevices, such as the cutting slide and the holes for the Kirschner wires. An explanation for this can be that Trios 3D scanners are based on confocal laser scanning technology. A 3D model can be reconstructed by taken successive images at

different focuses and aperture values and from different angles around the object (25). The scanner uses a laser to scan objects. The sensor registers the reflection of the laser on the object in the scanner. For small holes and small crevices, the laser light will probably not reflect on the surface of the 3D model due to the angulation of the scanner relative to the surface of the hole. Therefore, in this thesis, laser scanning spray was used for the small crevices. The spray dulls the surface of any shiny or reflective part. Applying the 3D scanner spray allowed the scanner to detect the small crevices. However, the application of 3D scanner spray in the small holes did not result in scanning its true dimensions since a thin layer had to be added. The average particle size of the fine-grained structure in this spray is 2.8 µm, which can impact the trueness of the measurements. On the contrary, this scanner spray was used both times before the models were scanned, meaning before and after the sterilization procedure. Therefore, the effect of the presence of the spray in the small crevices could not have resulted in large deformations when pre- and post-sterilization models were compared, as was done in this thesis.

In previous research conducted by Marei et al., the effect of steam sterilization on the dimensional changes of 3D printed surgical guides was investigated (26). The author concluded that steam sterilization did not significantly influence the dimensional changes and could thus be used as a valid method for sterilizing these 3D printed models. In this thesis, the results also indicate that the effect in terms of dimensional changes is minimal. To determine the accuracy of the printing process on its own, the digital STL file was also compared to the 3D printed result. Table 17 summarizes the dimensional differences between the digital STL file and the printed 3D BioMed Clear models. Some leftover marks remained on the 3D printed models' surface, as shown in Figure 25. The red dots indicate areas where the 3D printed model's surface is located outside of the digital STL file's surface and vice versa for blue areas. The unsupported surface of the model barely has any leftover marks from the printing process. Only on the top of the cutting slit where a thin red line is visible, which is marked with a black arrow. An explanation for this can be the leftover marks from the 3D scanning spray, which was hard to remove in the small areas. Overall, it is recommended to carefully choose the surgical guide's print orientation on the build platform. The guide's surface area that will contact the patient's bone must have a tight fit to prevent movement or incorrect placement. Therefore, the model should be orientated on the build platform so that this surface area is not in direct contact with the supports for printing. It is also recommended to minimize the amount of support in the drill- and cutting guides as these areas are hard to reach for the removal of the support structures. Unsatisfactory removal of the support structures in these areas could lead to inaccuracies during surgery and miss out on the surgical guide's goal. At Materialise (Materialise NV, Leuven, Belgium), a standard accuracy of ± 0.3% (0.3 mm) is accepted for polyamide 12 printed models that can be used as surgical guides. For BioMed Clear specimens, the mean and standard deviation values in Table 17 indicate that the accuracy of the Form 2 printer is more or less comparable to the standard accuracy provided by Materialise. The models' minimal and maximal deviations in dimensions can be determined by the mean ± 3σ, as 99.7% of the measured values will be within this range.

Table 17. A summary of the dimensional difference values between the original STL file and the printed models. CI stands for confidence interval.

Model	Mean ± CI [µm]	Standard deviation [µm]	Minimum [mm]	Maximum [mm]
1	22.17 ± 0.87	91.60	-0.40	0.498
2	71.51 ± 1.15	127.08	-0.48	0.819
3	22.56 ± 0.87	91.54	-0.38	0.497
4	31.48 ± 0.90	97.87	-0.67	0.499
5	20.42 ± 0.82	87.86	-0.38	0.497

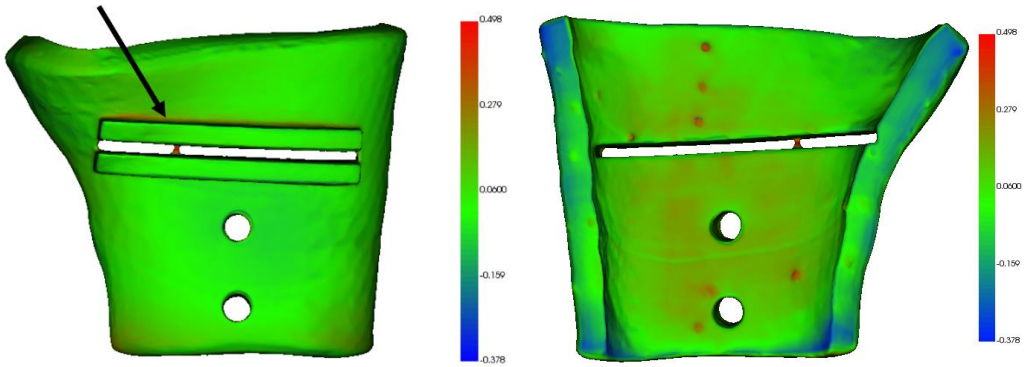

Figure 25. Distance heat map of model 5. Here the digital STL file is compared with the 3D printed model. The red dots are leftovers from the support structure that was used for printing.

The design of the surgical guide must be compatible with several design guidelines. For PA12 surgical guides manufactured by Oceanz, the minimal wall thickness is 0.7 mm. A higher wall thickness will result in a firm, solid surface, while a lower wall thickness creates a flexible surface. For BioMed Clear surgical guides, the minimal wall thickness should be investigated in future studies. Another factor that should be carefully addressed when designing surgical guides is the guide's contact area with the patient's bone. It is recommended that this area be sufficiently large so that shifting the surgical guide during operational procedures is minimized. The effect of shifting can be reduced by designing the guide so that the contact area covers some curvy structures for more grip. However, it must be taken into account that the guide does not contain curved regions of more than 90 degrees relative to the direction of placement, as this could limit the process of sliding the guide over the bone. The stability of guide positioning was investigated by Van den Broeck et al. (27). This paper explains that the stability of the guide depends on the contact point locations and can be evaluated from the coordinates and normal of the 3D contact points. Additionally, it is recommended that the design of the surgical guide does not contain any large, flat surfaces.
In most cases, the model will deform during printing and after the post-processing steps. Moreover, for BioMed Clear resin models, it is recommended to print the models at a 45° angle relative to the build platform. This minimizes the effect of warping and ensures good mechanical material properties. When designing the surgical guide, it is essential to maintain enough distance between the two parts, the target bone and the surgical guide. A perfect fit in the design CAD software does not necessarily result in a perfect fit during the operational procedure. Therefore, according to pre-operative planning specialists from Radboudumc (Nijmegen, The Netherlands), it is recommended to always leave at least 0.1 mm between the guide and the bone to compensate for small deformations and the presence of soft tissue.

An additional experiment was performed to compare the effect of steam sterilization on the dimensional changes of two different groups, namely BioMed clear specimens and PA12 specimens. Two different STL files were printed with each material. The files were based on the design of a patient-specific surgical cutting and drilling guide shown in figure 26. Both models were 3D printed with BioMed Clear resin with the Form 2 printer at the in-house 3D lab and with Polyamide 12 at Oceanz (Oceanz, Ede, The Netherlands). The specimens were scanned with a Trios 3D scanner before and after steam sterilization (134 °C for 3.5 minutes). The resulting STL files from the 3D scanner were compared in Slicer 3D. This method is previously elaborated in Part B of this thesis.

Figure 26. 3D models of a surgical drill guide on the left and a surgical cutting guide on the right. Both models were printed in BioMed Clear resin and in Polyamide 12 for dimensional tests. When opened in Word, models can be visualized in 3D.

The results are shown in a boxplot in Figure 27, and the descriptive statistics are summarized in Table 18. Overall, it can be seen that the range of dimensional deviations is less for PA12 3D printed models compared to BioMed Clear specimens. The deviation in dimensions due to the sterilization process for PA12 specimens was ± 0.105 mm compared to ± 0.234 mm for BioMed Clear specimens. Values were calculated by averaging the standard deviation for models printed with the same material. This indicates that sterilization has a larger effect on BioMed Clear specimens compared to PA12 specimens. The most considerable deviations in dimensional accuracy were seen in the specimens' small crevices where it was hard to reach with the 3D scanner. Therefore, conclusions should not be drawn based on the minimal and maximum values for each model.

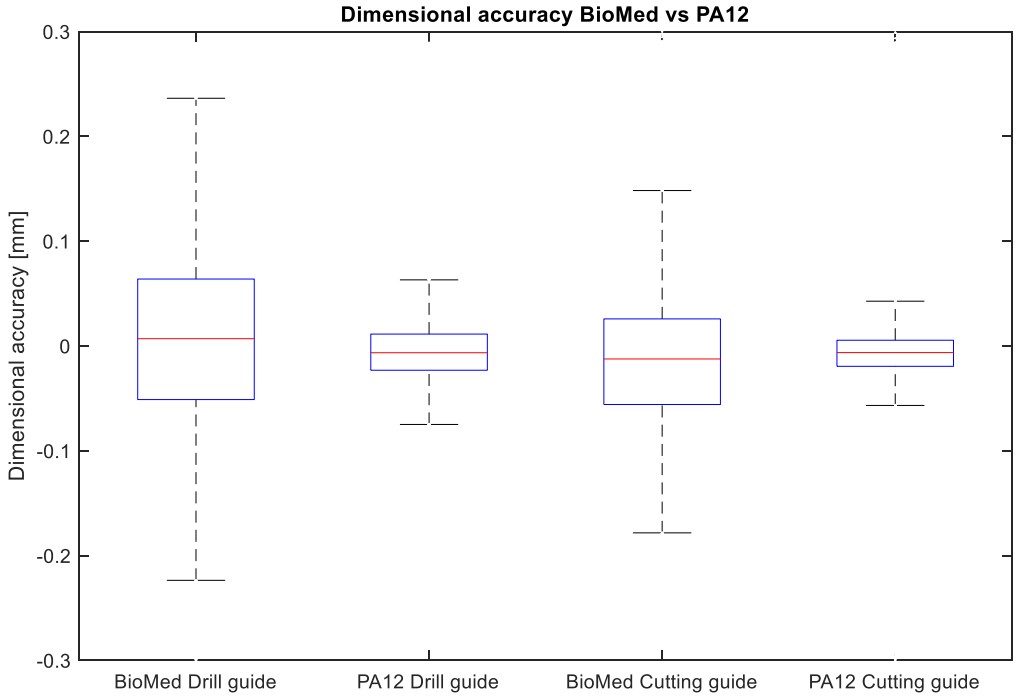

Figure 27. Boxplot showing the effect of steam sterilization on the dimensional accuracy of two different 3D print materials.

Table 18. Summary of test results on the effect of sterilization on the dimensional changes of 3D printed models.

Model	Mean [μm]	Standard deviation [μm]	Minimum [mm]	Maximum [mm]
BioMed Drill	5.27	89.96	-0.42	0.29
PA12 Drill	-5.86	28.73	-0.17	0.29
BioMed Cut	-13.22	66.78	-0.40	0.51
PA12 Cut	-8.71	40.54	-1.02	0.97

To determine the differences in the print accuracy between PA12 and BioMed Clear specimens, the original digital STL model was compared to the 3D printed version in its pre-sterilization form. The test results can be seen in Figure 28, and descriptive statistics are shown in Table 19. The results suggest that 3D printed PA12 specimens are more accurate to the original digital STL file compared to BioMed Clear specimens. The deviations in dimensions for 3D printed PA12 specimens compared to the original STL file were ± 0.156 mm compared to ± 0.284 mm for BioMed Clear specimens. This suggests that PA12 specimens can be printed almost twice as accurately by Oceanz compared to in-house printing with the Form 2 printer. However, the deviations in dimensions of BioMed Clear specimens remain within the lower limit of standard accuracy provided by Materialise (± 0.3 mm). Therefore, it might still be a suitable alternative to print the guides in-house with the Form 2 printer.

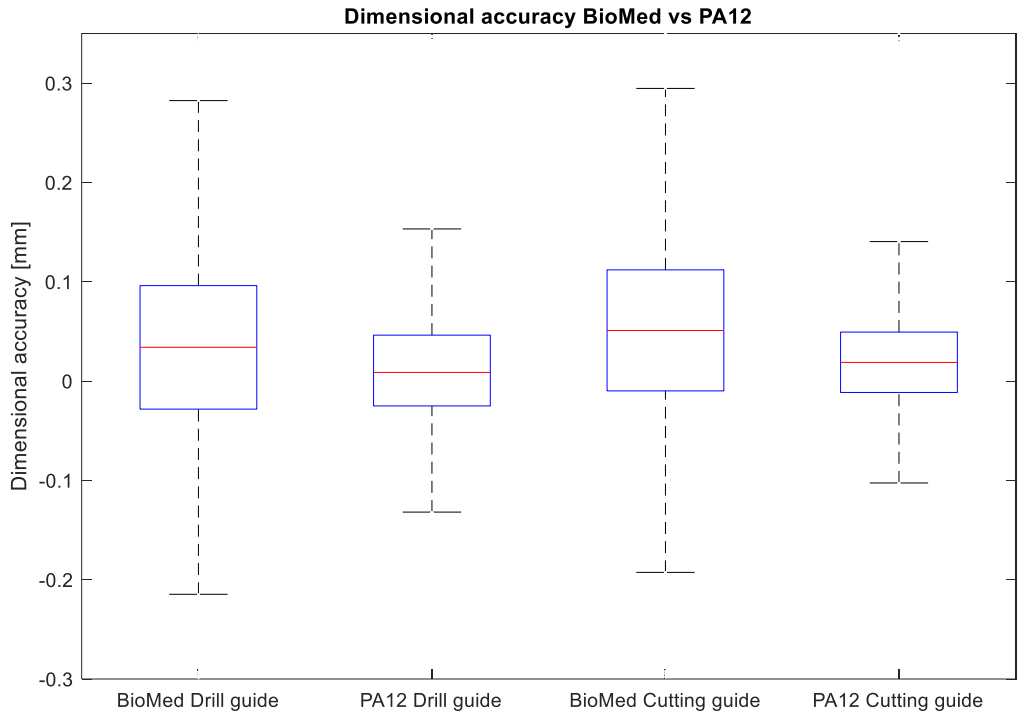

Figure 28. Boxplot showing the differences in dimensional deviations between the original digital STL model and the resulting 3D printed model.

Table 19. Summary of test results on the effect of sterilization on the dimensional changes of 3D printed models.

Model	Mean [μm]	Standard deviation [μm]	Minimum [mm]	Maximum [mm]
BioMed Drill	32.49	93.09	-0.73	0.62
PA12 Drill	11.29	56.55	-0.20	0.63
BioMed Cut	51.40	96.13	-0.41	0.65
PA12 Cut	20.60	47.41	-0.19	0.48

Sterility tests

In Part C of this thesis, the effect of in-house steam sterilization on bacterial contamination of BioMed Clear models was tested. Five different workflows were examined. Among the models in workflow C1 and C5 that were tested on bacterial contamination directly after the printing process, 9/10 models showed bacterial contamination. In almost all of the tested models in these groups, the bacterial contamination likely originated from the human skin flora, indicating unsterile processing of the specimens. Therefore, to ensure that the chance of bacterial contamination on the models is minimized, sterilization is mandatory. The goal of testing these workflows was to examine how sterile the production process and post-processing steps for both printers were. The models printed with the SLA printer were post-processed in IPA to remove any uncured resin. Additionally, IPA also works as a disinfectant to remove most of the bacterial contamination. While disinfection is the process of reducing or eliminating harmful microorganisms from objects or surfaces, sterilization is the process of killing all microorganisms, including bacterial spores. These spores could thus still have been present on the models after disinfection of the SLA printed models. Another explanation for the presence of bacteria on the models in group C1 and C5 is that these were processed in the 3D lab 'as sterile as possible.' Sterile gloves were used; however, there was no flow cabinet, and models had to be air-dried at room temperature before they could be placed in laminate pouches. This increased the chance of contamination.

MALDI-TOF MS was used for species identification of microorganisms cultured from AGAR plates. The results of this thesis show that this technique is a robust method to identify a vast majority of bacterial and fungal species. Although bacterial identification worked very well overall, some bacteria could not be identified to the respective species as the score value was below 2.000. An explanation for this can be the lack of reference spectra in the database or the species' rareness. However, the use of MALD-TOF MS is highly reproducible for bacterial identification as several studies have been published where the technique outperformed conventional microbiologic techniques (28). Conventional methods normally result in more incorrect genus-level identifications compared to MALDI-TOF MS (29).

Models in group C2, C3, and C4 were sterilized according to the hospital's protocol for steam sterilization. As a result, 14/15 models did not show any contamination after the sterilization procedure, indicating its efficacy. Models in group C3 were consciously contaminated with *S. Aureus* to ascertain whether it would still be present on the models after steam sterilization. Bacterial contamination tests using MALDI-TOF MS showed that the sterilization procedure was capable of eliminating *S. Aureus* from the 3D printed models. However, one model in group C3 was contaminated with bacteria, *cutibacterium species,* which is a non-pathogenic bacteria that most likely originated from the human skin flora. A possible moment of contamination can be during the models' processing steps at the Microbiology Department, where the models were processed in flow cabinets with sterilized instruments. Although the goal during this process is to work as sterile as possible, it is possible that the models got contaminated during these steps.

Laws and regulations

Internal production

The Medical Device Regulation (MDR) is a regulation of the European Union regarding the clinical investigation and sale of medical devices for human use. According to Article 5 of the MDR, healthcare institutions may manufacture and use medical devices within their organization if it can justify in its documentation that the target patient group's specific needs cannot be met by an equivalent device available on the market. As patient-specific surgical guides are custom-made medical devices, there will be no devices available on the market that can comply with their specific needs. Internally manufactured medical devices are exempt from the regulations' requirements, except the general safety and performance requirements in Annex I of the MDR, as long as they are not transferred to another legal entity. However, healthcare institutions must: apply an appropriate quality management system to manufacture and use the devices; draw up documentation regarding the manufacturing process; evaluate the design and performance data of the device, including the intended purpose; and review experiences gained from clinical use and take necessary corrective actions.

The quality management system (QMS) covers all healthcare institutions' organization elements that deal with the quality of the process, procedures, and devices. The system aids in giving structure to the organization in terms of responsibilities, structure, and processes necessary to comply with the MDR. Examples of aspects that must be addressed in the QMS are: product realization, including planning, design, development, production, and service provision; requirements for post-market surveillance; and data analysis of measurement output and product improvement. In ISO 13485, additional insights into the QMS are provided. In case the healthcare institution wants to make the medical device available on the market, the medical device's production process should be certified according to ISO 13485. This is a time-consuming process that requires some investment.

The production process of patient-specific surgical guides must be validated according to several factors. First, the combination of the material with the design of the surgical guide must be validated for a specific type of sterilization. Additionally, another validation has to be conducted to determine whether the 3D printed surgical guides are within the tolerance limit concerning the digital design in the form of an STL file. In this thesis, the effect of steam sterilization on the dimensional accuracy of 3D printed Biomed Clear surgical guides were investigated. Results in this thesis show that the standard accuracy of the Form 2 3D printer is comparable to the gold standard for printing patient-specific surgical guides, PA12. Moreover, the effect of in-house steam sterilization on the dimensional changes of 3D printed BioMed Clear models is ± 0.12 mm. This value is based on three times the maximum standard deviation from table 10.

Material requirements

To determine whether BioMed Clear resin is suitable as a material for the production of patient-specific surgical guides, it must also be biocompatible with the human body. The biocompatibility or biological evaluation of medical devices can be investigated according to the ISO 10993 standard. In this standard, the biological evaluation of sterile and non-sterile medical devices that come into direct or indirect contact with the human body is specified. The ISO standard lists recommended tests based on the type and duration of body contact. According to Attachment A of this standard, a medical device that is in contact with human bone or tissue for less than 24 hours should be tested on biocompatibility in terms of cytotoxicity, sensitization, irritation or intracutaneous reactivity, acute systemic toxicity, and materials-mediated pyrogenicity. Biocompatibility testing must be completed on the finished device. In the case of a surgical guide, this would mean that the specimens must be sterilized before biocompatibility tests.

BioMed Clear Resin specimens have been tested following ISO 10993-1:2018 at NAMSA World Headquarters (Northwood, OH, USA). The material has passed the requirements for the following biocompatibility risks: not cytotoxic, not a sensitizer, not an irritant, not toxic, and not genotoxic. Moreover, BioMed Clear is a USP (U.S. Pharmacopeial

Convention) Class VI certified material, which means that the material has passed the most stringent biocompatibility tests for plastics and polymers used in medical devices in the United States. To get the USP class VI certification, the material must be compatible with various tests such as; systemic injection test, intracutaneous test, and implantation test. It is not clear whether BioMed Clear Resin has passed the pyrogenicity tests for biocompatibility according to ISO 10993-11, as this is not mentioned in the material properties data provided by Formlabs. This test evaluates the potential of the material to induce a pyrogenic response (fever). The FDA recommends that this test is performed for the application where the device will be in contact with bone and/or tissue for less than 24 hours.

Cost-benefit analysis

During this thesis, I assisted in the process of designing and printing a patient-specific surgical guide. The intention was to use the surgical guide in real-life during surgery of a distal radius correction osteotomy. However, due to the COVID-19 pandemic, the surgery was delayed and not performed within my thesis period. This patient-case was intended to be taken as an example of the expenses that come with the process of designing and printing such a patient-specific surgical guide. These costs of external production will be compared with the in-house production of the guides to determine whether it is beneficial.

The design of the guide was performed by experienced professionals from the medical 3D lab of the Radboudumc (Nijmegen, The Netherlands). It took them roughly 4-5 hours, resulting in €450 total cost for the design of the guides. The design of the guides was performed in Autodesk 3ds Max, which is a commercial software for 3D modeling and 3D animation. This software is free to download with a student license. The resulting three STL files were then printed at Oceanz (Ede, The Netherlands) in PA12. Two guides were designed for the distal radius as a drilling and cutting guide, and one guide was used to acquire a bone graft from the hip of the patient since it was planned to be an open wedge osteotomy. The total cost for printing the guides, including taxes, shipping, and a declaration of conformity, was € 91. Therefore, the total cost for designing and printing the guides via external companies was € 541. The benefit of designing a guide via an external company is that it is mostly performed by experienced professionals. These professionals know most of the tips and tricks for an efficient design process resulting in a reduction of the design phase time. Another benefit of outsourcing the printing process is that an external company like Oceanz has already certified its production process for surgical guides. This ensures that the delivered product is tested according to the ISO standards and safe for its application.

In this part, an estimation of the costs for the in-house production of surgical guides is performed. The price of BioMed Clear resin is €381,15 per liter. The models then cost €6,86 since printing them requires 18 mL of resin. In addition, the price of the printer, wash, and cure should be added to the total cost for the production. As an example, two situations are elaborated where the hospital will perform five and eight surgical procedures a year over a period of 10 years where patient-specific surgical guides will be used. These guides will be manufactured in-house with the Form 2 printer. In Table 20, the total costs for producing these guides over a period of 10 years are summarized.

Table 20. The total cost of production for surgical guides with 5 cases a year over a period of 10 years.

Product	**Cost/product**	**5 surg./year**	**8 surg./year**
Surgeries in 10 years		50	80
Labor costs per print[a]	€ 3.44	€ 172	€ 275.20
Variable costs[a] *(e.g. electricity, maintenance)*	€ 2.20	€ 110	€ 176
Form 2 printer	€ 3000	€ 3000	€ 3000
Form Wash	€ 500	€ 500	€ 500
Form Cure	€ 700	€ 700	€ 700
Resin tank LT	€ 80	€ 800	€ 800

Isopropyl alcohol (20 liter)	€ 120	€ 1200	€ 1200
BioMed Clear (1 liter)	€ 380	€ 380	€ 760
Average price per case		€ 137.24	€ 92.64
Total price		€ 6862	€ 7411.20

[a] *Labor and variable costs are estimated based on a tool provided by Formlabs for the determination of Return on Investment and to calculate time and cost-savings.*

The labor costs and variable costs are estimated with the use of a tool provided by Formlabs to determine the time and cost-savings when 3D printing on the Form 2 is compared to alternative production methods (30). As an example for the determination of the costs, the production of a biocompatible patient-specific surgical guide in dentistry is used. According to Formlabs, the labor costs for the production of a single print are $ 4.17 (€ 3.44), and the variable costs are $ 2.67 (€ 2.20). The labor costs are based on $ 25 per hour (€ 20.60). The prices in Table 19 are based on five and eight surgeries per year over a period of ten years. For a total of 50 surgeries, the average price for the production of the guides will be €137,24 per case. In order to compete with the cost of surgical guides provided by Oceanz, the hospital should perform on average more than eight surgeries a year over a period of 10 years where patient-specific surgical guides will be used (€92.64 per case). The highest costs for the production of patient-specific surgical guides are made in the design phase (€450). Therefore, a more obvious first step to lower the costs and improve the efficiency of the whole process would be to insert this phase into the hospital's workflow. This requires dedicated software and training of personnel to work with the software. When the design phase is taken into the hospital's workflow, the whole process from taking a CT-scan from a patient to the eventually designed guide will be more efficient and accessible.

Conclusion and future perspective

The current workflow for the design and production of patient-specific surgical guides at the Elisabeth-Two Cities hospital is out-sourced to external companies. This results in a time-consuming and costly process. Furthermore, the hospital features a laboratory with 3D printers and dedicated software that could possibly take over the tasks of producing the guides in-house. The aim of this thesis was to investigate whether the in-house available desktop 3D printers would be suited for the production of these surgical guides. Therefore, the guides must be compatible with the in-house sterilization method.

The effect of in-house steam sterilization on the mechanical, dimensional, and sterility properties of a novel biocompatible 3D print material, BioMed Clear resin, was investigated. The results of the mechanical tests suggest that BioMed Clear specimens are stronger and stiffer compared to the current gold standard material for the production of patient-specific surgical guides, polyamide 12. The effect of sterilization on the dimensional properties of BioMed Clear specimens combined with the standard print accuracy is comparable to the tolerance limit provided by other surgical guide manufacturers. However, PA12 seems to deform less due to sterilization when directly compared to BioMed Clear. Additionally, the sterility tests indicate that the material is suitable to be sterilized by the in-house sterilization method. Moreover, specimens stored in the sterile storage area also remained sterile over a period of four weeks, indicating the efficacy of the process and packaging.

The development of more automatic software for pre-operative planning, together with the rapid growth in the additive manufacturing industry, could open the door to in-house 3D printing facilities in hospitals, which would increase the availability of personalized instrumentation. In terms of research purposes, the in-house printing of patient-specific surgical guides is thought to be achievable with respect to the new Medical Device Regulations as of May 2021. However, in case a hospital repeatedly uses the same application, they can out-source this to certified companies as otherwise, they take on the role of the specialized manufacturer, while the focus should be on research and innovations that contribute to better care for patients and possibly also to lower costs. For now, it is recommended to design the surgical guide in-house to allow for direct consultation and feedback from the operating surgeon. Also, it is recommended to out-source the printing process to certified companies like Oceanz since their production process is proven to be tested in a quality management system. In case the hospital wants to produce the guides in-house, it must comply with an appropriate quality management system, document the manufacturing process, evaluate the performance, and review experiences from clinical use.

Bibliography

1. CBS. Operaties in het ziekenhuis; soort opname, leeftijd en geslacht, 1995-2010 2014 [Available from: https://opendata.cbs.nl/statline/#/CBS/nl/dataset/80386ned/table?ts=1593158155387.
2. Rutala WA, Weber DJ. Disinfection and sterilization: an overview. Am J Infect Control. 2013;41(5 Suppl):S2-5.
3. Rutala WA, Weber DJ, HICPAC. Guideline for disinfection and sterilization in healthcare facilities. Centers for Disease Control and Prevention. 2008.
4. Spaulding E. Chemical disinfection of medical and surgical materials. Lawrence C, Block SS, eds Disinfection, sterilization, and preservation. 1968;517-31.
5. Rutala WA, Weber DJ. Disinfection and Sterilization in Health Care Facilities: What Clinicians Need to Know. Clinical Infectious Diseases. 2004;39(5):702-9.
6. WHO. Decontamination and reprocessing of medical devices for health-care facilities. 2016.
7. Redwood B. Medical 3D printing applications. Available from: https://www.3dhubs.com/knowledge-base/medical-3d-printing-applications/ [July 2020].
8. Baumers MH, M. Rowley, J. . The economics of 3D printing: a total cost perspective. 2016. https://www.ifm.eng.cam.ac.uk/uploads/Research/TEG/3DP-RDM_Total_cost_report.pdf (data last accessed 19 January 2021).
9. Crafts TD, Ellsperman SE, Wannemuehler TJ, Bellicchi TD, Shipchandler TZ, Mantravadi AV. Three-Dimensional Printing and Its Applications in Otorhinolaryngology–Head and Neck Surgery. Otolaryngology–Head and Neck Surgery. 2016;156(6):999-1010.
10. Cui H, Nowicki M, Fisher JP, Zhang LG. 3D Bioprinting for Organ Regeneration. Adv Healthc Mater. 2017;6(1).
11. Marro A, Bandukwala T, Mak W. Three-Dimensional Printing and Medical Imaging: A Review of the Methods and Applications. Curr Probl Diagn Radiol. 2016;45(1):2-9.
12. Shaheen E, Alhelwani A, Van De Casteele E, Politis C, Jacobs R. Evaluation of Dimensional Changes of 3D Printed Models After Sterilization: A Pilot Study. Open Dent J. 2018;12:72-9.
13. Formlabs. Moving from FDM to SLA: Part 1. Available from: https://formlabs.com/blog/how-to-orient-sla-parts/#Drainage. Accessed 21 January 2021.
14. Song M, Tao D, Sun S, Chen C, Maybank SJ. Robust 3D face landmark localization based on local coordinate coding. IEEE Trans Image Process. 2014;23(12):5108-22.
15. Emonet S, Shah HN, Cherkaoui A, Schrenzel J. Application and use of various mass spectrometry methods in clinical microbiology. Clin Microbiol Infect. 2010;16(11):1604-13.
16. Fenselau C, Demirev PA. Characterization of intact microorganisms by MALDI mass spectrometry. Mass Spectrom Rev. 2001;20(4):157-71.
17. Clark AE, Kaleta EJ, Arora A, Wolk DM. Matrix-assisted laser desorption ionization-time of flight mass spectrometry: a fundamental shift in the routine practice of clinical microbiology. Clin Microbiol Rev. 2013;26(3):547-603.
18. Di Vona ML. Annealing of Polymer Membranes. In: Drioli E, Giorno L, editors. Encyclopedia of Membranes. Berlin, Heidelberg: Springer Berlin Heidelberg; 2016. p. 1-2.
19. Butt, J.; Bhaskar, R. Investigating the Effects of Annealing on the Mechanical Properties of FFF-Printed Thermoplastics. J. Manuf. Mater. Process. 2020, 4, 38. https://doi.org/10.3390/jmmp4020038.

20. Wang S, Daelemans L, Fiorio R, Gou M, D'Hooge D R, De Clerck K, et al. Improving Mechanical Properties for Extrusion-Based Additive Manufacturing of Poly(Lactic Acid) by Annealing and Blending with Poly(3-Hydroxybutyrate). Polymers (Basel). 2019;11(9).
21. Abhari RE, Mouthuy P-A, Zargar N, Brown C, Carr A. Effect of annealing on the mechanical properties and the degradation of electrospun polydioxanone filaments. Journal of the Mechanical Behavior of Biomedical Materials. 2017;67:127-34.
22. Materialise. Polyamide 12 (SLS) - Technical specifications and datasheet. Available from https://www.materialise.com/en/manufacturing/materials/pa-12-sls Accessed 21 january 2021.
23. Formlabs. BioMed Clear material properties data. Available from https://formlabs-media.formlabs.com/datasheets/2001432-TDS-ENUS-0.pdf. Accessed 21 January 2021.
24. Ballard DH, Mills P, Duszak R, Jr., Weisman JA, Rybicki FJ, Woodard PK. Medical 3D Printing Cost-Savings in Orthopedic and Maxillofacial Surgery: Cost Analysis of Operating Room Time Saved with 3D Printed Anatomic Models and Surgical Guides. Acad Radiol. 2020;27(8):1103-13.
25. Richert R, Goujat A, Venet L, Viguie G, Viennot S, Robinson P, et al. Intraoral Scanner Technologies: A Review to Make a Successful Impression. Journal of Healthcare Engineering. 2017;2017:8427595.
26. Marei HF, Alshaia A, Alarifi S, Almasoud N, Abdelhady A. Effect of Steam Heat Sterilization on the Accuracy of 3D Printed Surgical Guides. Implant Dent. 2019;28(4):372-7.
27. Van den Broeck J, Wirix-Speetjens R, Vander Sloten J. Preoperative analysis of the stability of fit of a patient-specific surgical guide. Comput Methods Biomech Biomed Engin. 2015;18(1):38-47.
28. Dingle TC, Butler-Wu SM. MALDI-TOF Mass Spectrometry for Microorganism Identification. Clinics in Laboratory Medicine. 2013;33(3):589-609.
29. van Veen SQ, Claas ECJ, Kuijper EJ. High-Throughput Identification of Bacteria and Yeast by Matrix-Assisted Laser Desorption Ionization-Time of Flight Mass Spectrometry in Conventional Medical Microbiology Laboratories. Journal of Clinical Microbiology. 2010;48(3):900.
30. Formlabs Inc., Your 3D printing Return On Investment report. Available from; https://formlabs.com/roi/ Accessed on 10-02-2021.